8

RADIOACTIVE DATING METHODS

R. BOWEN

INTRODUCTION

Radioactive dating methods involve radioactive isotopes of various elements and, of the 1400 to 1500 nuclides known presently, more than four-fifths are radioactive although most of them do not occur naturally because of their very rapid rates of radioactive decay. To obtain the ages of rocks and minerals, naturally occurring radioisotopes are used which continued to exist long after the Big Bang because of their extremely slow decay rates. This is the case with ^{238}U, ^{235}U, ^{232}Th, ^{87}Rb and ^{40}K. However, some arise from the decay of long lived, naturally occurring radioactive parents, among them ^{234}U, ^{230}Th and ^{226}Ra. And a few may be created by natural nuclear reactions, for instance ^{14}C (radiocarbon), ^{10}Be and ^{3}H (tritium). While today, artificial radioisotopes have been introduced into the environment by thermonuclear testing and the operation of nuclear fission reactors and particle accelerators. Whatever its source, radioactivity is significant with regard to geochronology and radioactive dating researches really began in an attempt to determine the age of the Earth. This was not long after Henri Becquerel's discovery of it in 1896 and the work of Marie Curie who found that thorium and uranium minerals emit radiation and later identified two new elements, polonium and radium. In fact, it is from the latter that the word "radioactivity" derived. So by 1913, it became possible for serious investigations to be made regarding our planet's age, a matter referred to by Arthur Holmes as indelicate, adding that they were in progress anyhow because "Science knows no shame". Subsequently, dramatic developments have taken place and determining the ages of minerals, rocks, archaeological and historical objects and so on is now routine. The major methods for achieving this are discussed in this chapter of which the main aim is to provide a brief perspective of the subject which is actually vast in scope. These are listed alphabetically and include four radiation damage techniques which are electron spin resonance, fission track dating, pleochroic haloes and thermoluminescence. No effort has been made to describe new approaches still being developed such as the La/Ce isotope scheme which constitutes a potentially powerful adjunct to the Sm/Nd method for petrogenetic studies but which is impeded because of the conflict between the best determination by counting of the β-decay half-life of La (3.02×10^{11} a^{-1}) and geological half-life assessments based on La/Ce and Sm/Nd mineral isochrons. In addition, it has been necessary to exclude information apropos recent research progress because of space restrictions. Also because readers will have different scientific requirements and most may not be involved in radiometric dating concerned with changes in the radioactivities of samples. Anyone interested in acquiring more detailed knowledge can consult the author's "Isotopes in the Earth Sciences" (Chapman & Hall, London, 1994) or a second edition of this now prepared and published in 1997 called "Radioactive and Stable Isotope

R. BOWEN • Just retired from Wilhelms University, Münster 21 Kings Gardens, Huntington, Cambs PE18 7LL, England

Nuclear Methods in Mineralogy and Geology: Techniques and Applications
Edited by Vértes *et al.*, Plenum Press, New York, 1998

Geology" which has a co-author, H.-G. Attendorn, and published by Chapman & Hall. Nevertheless this chapter offers a useful and compact synopsis of radioactive dating methods for non-specialist professionals and moreover for students of the earth sciences too.

8.1. ARGON/ARGON

8.1.1. Methodology

Excess radiogenic argon may occur in minerals and produce K/Ar dates which are too old. $^{40}Ar/^{39}Ar$ dating aimed at overcoming this problem. It is based on the formation of ^{39}Ar by irradiation of potassium-bearing minerals using thermal and fast neutrons in a nuclear reactor, the reaction being $^{39}_{19}K(n,p)^{39}_{18}Ar$. ^{39}Ar is a radioactive nuclide which decays to ^{39}K by beta emission with $T_{1/2}$=269 a. The decay rate is sufficiently slow for ^{39}Ar to be regarded as stable for the relatively short analytical time. The number of radiogenic ^{40}Ar atoms in a sample due to the radioactive decay of ^{40}K during its geological history is given by:

$$^{40}Ar = \frac{\lambda_{ec}}{\lambda} {}^{40}K(e^{\lambda t} - 1) \tag{8.1.1}$$

where λ_{ec} is the decay constant of ^{40}K for e.c. and λ is the total decay constant.* After neutron irradiation, a value for the $^{40}Ar/^{39}Ar$ ratio may be obtained and utilized to calculate a date thus:

$$t = \frac{1}{\lambda} \ln\left[\frac{^{40}Ar}{^{39}Ar} \cdot J + 1\right]$$

where t = time and J is a parameter derived from:

$$J = \frac{e^{\lambda t}_{fm} - 1}{\left(^{40}Ar/^{39}Ar\right)_{fm}}$$

where t_{fm} is the known age of the flux monitor used the isotope ratio of which is $(^{40}Ar/^{39}Ar)_{fm}$. As a matter of course the monitor is irradiated with the same neutron flux and for the same time as the sample itself and the amount of ^{39}K does not change appreciably during irradiation. Various mineral concentrates have been employed as flux monitors and their ages are accurately known. Assumptions are that all ^{40}Ar in the irradiated sample is either radiogenic or atmospheric in origin, that all ^{36}Ar is atmospheric and that ^{39}Ar is produced by the (n,p) reaction. If this were so, the measured values of the $^{40}Ar/^{39}Ar$ and $^{36}Ar/^{39}Ar$ ratios would enable the desired ratio of radiogenic ^{40}Ar to ^{39}Ar to be calculated thus:

$$\frac{^{40}Ar}{^{39}Ar} = \left(\frac{^{40}Ar}{^{39}Ar}\right)_m - 295.5\left(\frac{^{36}Ar}{^{39}Ar}\right)_m \tag{8.1.2}$$

where m = measured values and 295.5 is the ratio between ^{40}Ar and ^{36}Ar in atmospheric Ar. Ar has 15 isotopes of which at least 5 result from interactions between neutrons and the isotopes of K, Ca and Cl, this necessitating corrections particularly important as regards young samples (~10^6 a) and those where K/Ca<1.0.

Clearly a date can be calculated from the $^{40}Ar/^{39}Ar$ ratio of a sample which has been irradiated by neutrons and a set of such dates can be obtained if Ar is liberated from the sample in steps, a procedure discussed below [1].

---

*^{40}K also undergoes β^{-5} decay and therefore $\lambda=\lambda_{ec}+\lambda_{\beta-}$

8.1.2. Incremental heating

If a sample was a closed system for Ar and K since it cooled, the dates derived from each heating step should be constant. However, if some radiogenic Ar was lost in respect of some crystallographic sites then the $^{40}Ar/^{39}Ar$ ratios of the gases released at different temperatures will vary and a range of dates will result from which the time elapsed since initial cooling may be obtainable. An appropriate model showed that such a stepwise heating procedure applied to a mineral sample which underwent partial loss of radiogenic Ar could yield such a range of dates by calculation and this might give the time of metamorphism (low temperature partial release of the gas) and the time of initial cooling (high temperature partial release of the gas), see Figure 8.1.1. The advantage was thought to be that it facilitated the deriving of a date nearing, if sometimes under-estimating, the original cooling age of potassium-bearing minerals which underwent partial loss of radiogenic ^{40}Ar during a metamorphic episode. The model was used to make cooling rate assessments of severely shocked chondrites [2].

An atmospheric ^{40}Ar correction is applied to both conventional K/Ar and $^{40}Ar/^{39}Ar$ dating methods, but it assumes that the ^{36}Ar is of atmospheric origin and that the $^{40}Ar/^{36}Ar$ ratio in the atmosphere is now 295.5 which it is. But ^{40}Ar and ^{36}Ar may become incorporated into minerals when they crystallize, hence the $^{40}Ar/^{36}Ar$ ratio of the gas may be significantly different from that of atmospheric Ar today. Thus, the observed quantity of ^{36}Ar in a mineral may not permit an

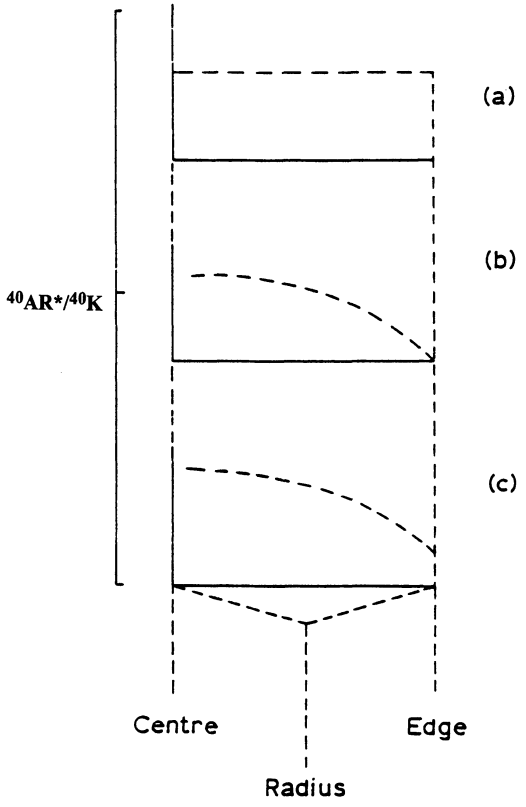

Figure 8.1.1. Schematic diagram showing a) the uniform distribution of the $^{40}Ar^*/^{40}K$ ratio in a spherical mineral grain comprising a closed system since crystallization; b) partial $^{40}Ar^*$ loss through diffusion induced by heating which reduced the relevant ratio to zero at the surface of the grain while leaving it unaltered at the center; c) the distribution of the $^{40}Ar^*/^{40}K$ ratio at a time after partial Ar loss after the system again became closed to $^{40}Ar^*$. The value of the $^{40}Ar^*/^{40}K$ ratio on the surface of the grain is a function of that time which elapsed subsequently to partial out-gassing and, at the center of the grain, it corresponds to the age of the mineral sample.

accurate correction to be made for the presence of non-radiogenic ^{40}Ar. Where the $^{40}Ar/^{36}Ar$ ratio of the inherited Ar exceeds 295.5, an apparent excess of radiogenic ^{40}Ar results. On the other hand, if the $^{40}Ar/^{36}Ar$ ratio of the inherited Ar is less than 295.5, there will be an apparent deficiency of radiogenic ^{40}Ar which might be attributed mistakenly to a partial loss of ^{40}Ar. An Ar isotope correlation diagram overcame the difficulty. It showed that the measured $^{40}Ar/^{36}Ar$ ratios obtained from gas fractions liberated during stepwise heating of an irradiated sample (after correction for interfering reactions) may be expressed thus:

$$\left[\frac{^{40}Ar}{^{36}Ar}\right]_m = \frac{^{40}Ar_c + ^{40}Ar}{^{36}Ar_c} \qquad (8.1.3)$$

where c refers to contaminant Ar (including the atmospheric component as well as Ar either occluded during crystallization of the mineral or entering it at a later stage). Suitably rewritten to take account of Ar produced by K in the sample, the equation represents a group of straight lines in coordinates of $^{40}Ar/^{36}Ar$ and $^{39}Ar/^{36}Ar$ (measured) with slopes equalling the $^{40}Ar/^{39}Ar$ ratio. Consequently, the measured $^{40}Ar/^{36}Ar$ and $^{39}Ar/^{36}Ar$ ratios of the incremental gas fractions freed from an undisturbed mineral will define a set of points fitting a straight line, i.e. an isochron, of which the slope is the $^{40}Ar/^{39}Ar$ ratio and relates to the age of the sample *t*, of equation 8.1.1. The intercept of the isochron will be the $^{40}Ar/^{36}Ar$ ratio of the contaminant, i.e. the ratio of these isotopes in the non-radiogenic gas fraction which is associated with the sample which is being analyzed. It may be added that often the initial $^{40}Ar/^{36}Ar$ ratio does not differ appreciably from the present atmospheric value of 295.5.

There is a possibility that ^{39}Ar may either be lost or relocated in a sample because of recoil of the ^{39}K nucleus due to the emission of a proton in the course of the (n,p) reaction. If an appreciable amount is lost from an irradiated sample, the $^{40}Ar/^{39}Ar$ ratio will increase proportionally and the total release date obtained will be older than the actual geological age. Loss of ^{39}Ar from a potassium-bearing mineral may occur from a surface layer *ca* 0.08 μm thick and the effect is related to the particle size of the mineral. Fractured or fine-grained minerals lose more ^{39}Ar during irradiation than do coarse-grained ones. Serious implications arise, among them that the $^{40}Ar/^{39}Ar$ method may be inapplicable to dating potassium-rich clay minerals of the glaucony type which usually comprise green pellets composed of aggregates of platey minerals *ca* 1 μm thick. For instance, very old total release $^{40}Ar/^{39}Ar$ dates for early Ordovician glaucony from Vastergotland, Sweden, were recorded and associated conventional K/Ar dates were approximately 8% lower than the known geological age.

It is important to recognise excess ^{40}Ar which is that ^{40}Ar that became incorporated in minerals through processes other than the *in situ* radioactive decay of ^{40}K. It must be distinguished from inherited Ar derived from precisely such radioactive decay prior to a rock-forming event involving minerals containing ^{40}Ar. Both excess and inherited Ar may be termed extraneous Ar. The conventional K/Ar dates of minerals which include excess ^{40}Ar exceed their cooling ages and are not valid determinations of ages. The incremental heating procedure is sometimes capable of discerning the presence of excess ^{40}Ar by means of a saddle-shaped spectrum of dates and similar patterns have been observed for biotite, pyroxene, hornblende and plagioclase from rocks known to contain such an excess. However, while these showed such an excess to exist, they did not help in establishing the age of the host material. It is interesting that biotites from metamorphic rocks known to have such excess ^{40}Ar gave partial release spectra with flat plateaux which exceed the known geological age of the rocks. In such cases, the incremental heating procedure cannot distinguish radiogenic ^{40}Ar formed by the radioactive decay of ^{40}K in the rock from excess ^{40}Ar added after crystallization. This is because the excess ^{40}Ar is distributed homogeneously in the sample with respect to the K in it. The inference is that the existence of a plateau in the spectrum of partial release dates of a sample is not necessarily indicative that its $^{40}Ar/^{39}Ar$ plateau is valid from a geological standpoint.

8.1.3. Argon release by laser

The $^{40}Ar/^{39}Ar$ age spectra of a whole rock sample and mineral concentrates may alter if they involve minerals that may lose Ar at a continuous rate even at low temperatures or minerals

younger than the main ones. These can result from episodes of thermal metamorphism at low temperature or may exist as inclusions in the main minerals. Either way, it is hard to separate them from the main minerals and, since they are characterized by their inability to retain Ar, their presence in irradiated samples contributes to low dates commonly derived from low temperature-derived gas fractions freed by incremental heating. The problem has been tackled by using a precisely focussed laser beam to release gas from individual grains of retentive minerals. One such grain can be selected and impinged on often enough to release enough Ar for isotope analysis. The gas is collected on charcoal at the temperature of liquid nitrogen and later a gas source mass spectrometer is utilized to obtain the $^{40}Ar/^{39}Ar$ ratio. Another technique involves applying continuous Ar-ion lasers to melt individual mineral grains previously irradiated by fast neutrons. Ar release using lasers is valuable because individual mineral grains can be dated so that their inclusions and any alteration products can be excluded. Also, it is possible to analyze several such grains in a rock sample and, by comparing the results, deduce the effects of temperature, pressure and alteration on the retention of Ar and K. In addition, polymictic breccias and similar rocks containing minerals of different ages can be examined without having to separate individual minerals (a task often hard or even impossible to carry out) [3].

The introduction of ultra-low background, ultra-sensitive inert gas mass spectrometers coincidentally with the development of the $^{40}Ar/^{39}Ar$ method offered new resolving power for geochronological studies. Later use of a continuous Ar ion laser fusion $^{40}Ar/^{39}Ar$ system permitted minute quantities (~1 mg) of potassium-rich geological materials to be dated with a precision nearing 0.2%. The approach has advantages over the K/Ar method and perhaps the greatest of these is that only ratios of Ar isotopes have to be measured in order to calculate an age rather than absolute amounts. As a result, it is not necessary to extract all radiogenic Ar from a mineral to derive an accurate age and this mitigates a problem inherent in the K/Ar dating of sanidine, i.e. that the K/Ar ages of this mineral tend to be anomalously young because the melt usually forms a viscous mass which retains some radiogenic Ar under ultra-high vacuum. Even at maximum attainable temperatures (1,800 °C) in standard RF-induction heaters and resistance furnaces, 5% to 10% of the gas can remain trapped in such viscous sanidine melts.

An interesting application of laser probe dating on potassium feldspar from the core of the Manson Impact Structure (USA) is important because this may have formed during Cretaceous-Tertiary boundary times and record a giant bolide impact thought to have led to the extinction of more than half of the species then living. At the 420.5 foot level, the sample proved consistent with conventional age spectrum total gas data from it at ~74 Ma. Other values ranged from *ca* 65 Ma to *ca* 97 Ma. Taking into account factors such as ^{39}Ar recoil during irradiation and the inclusion of incompletely degassed protolith material, a time of impact less than ~73 Ma was implied. A maximum age for the structure of 65.4±0.4 Ma was put forward. A similar age was obtained for the Chicxulub Structure (Mexico) which is regarded as another candidate for the impact which might have been caused by an asteroid [4,5].

8.2. CAESIUM-137/CAESIUM-135 AS A CHRONOMETER-TRACER

The natural caesium isotope ^{133}Cs (abundance 100%) is stable and there are 34 radioisotopes as well. The interesting isotopes are ^{135}Cs and ^{137}Cs. Both are radioactive with half-lives of 2.3 Ma and 30 a respectively. They are produced with equal yields of *ca* 6 to 7% in binary fission of actinide nuclides. Caesium nuclei enter the environment through atmospheric testing of nuclear weapons and release from nuclear industry. Cs-137 is a well known tracer and time marker whereas, according to Lee et al (1993) Cs-135 has been practically disregarded because its long half-life precludes detection by counting, also that, in conventional mass spectrometers, the tail from the stable caesium-133 swamps its signal (since its abundance is typically 10^{-9} smaller).

8.2.1. Application

Lee et al (1993) reported the first measurement of the caesium isotopes 133 (stable), fission 135 and fission 137 using two coastal sediment samples and a thermal ionization mass spectrometer equipped with a retarding potential quadrupole lens filter. The $^{135}Cs/^{133}Cs$ ratio was *ca* 1×10^{-9} and the $^{137}Cs/^{135}Cs$ was about 5 due to the decay occurring through the past 30 a from their

production ratio of *ca* 1. These authors noted that this appeared to be the first detection of fallout ^{135}Cs in nature, adding that the isotope ratio $^{137}Cs/^{135}Cs$ is much more powerful as a chronometer-tracer than ^{137}Cs on its own. They presented two models illustrating how the ratio may be employed in order quantatively to estimate recent sedimentation and rates of erosion.

8.3. COSMOGENIC RADIONUCLIDES

8.3.1. Aluminum-26

^{26}Al enters the oceans in ionic form and mixes with stable ^{27}Al, later becoming adsorbed on various particles. Its concentration rises with depth and its half-life is 0.716×10^6 a. Its residence time has been estimated at 1,400 a which make it valuable for dating authigenic minerals, although its detection is very difficult. It has been used to determine the rates of growth of manganese nodules of which one estimate is 2.3±1 mm Ma^{-1}. Where it is measured with beryllium-10 from the same sample, the ratio between their respective rates of radioactive decay decreases with time and it has been shown that:

$$\frac{^{26}Al}{^{10}Be} = \left[\frac{^{26}Al}{^{10}Be}\right]_i e^{-\lambda t}$$

so that the geochronometer is useful because the time-dependent variations in the rates of production and the geochemical paths of the two tend to annul each other [6].

8.3.2. Argon-39

This radionuclide forms in the atmosphere through the nuclear reaction $^{40}Ar(n,2n)^{39}Ar$ and decays by beta emission to ^{39}K with $T_{1/2}$ = 269 a. Its contribution to atmospheric radioactivity is *ca* 1.87±0.17 Bq m^{-3} and, of this, less than 5% is due to thermonuclear testing. It has a long residence time which damps down fluctuations in its production rate and contributes to probable constancy of its concentration in terms of time and latitude. This makes it useful for dating glacial ice and groundwater. At *ca* 70 m depth, névé is converted to glacial ice and air bubbles are entrapped which can be analyzed in order to assess disintegration rates for ^{39}Ar as well as for radiocarbon and ^{81}Kr. The main problem in employing it is its chemical inertness through which it does not interact with solids (unlike radiocarbon ^{32}Si and ^{36}Cl). And because it and other noble gas radioisotopes occur mostly in the atmosphere, concentrations in groundwater depend on the time elapsed since the water was in contact with the atmosphere. In addition, analysing ^{39}Ar entails collecting very large volumes of water as with ^{32}Si. Also excess ^{39}Ar may arise from the nuclear reaction $^{39}K(n,p)^{39}Ar$ in rocks containing measurable quantities of U and Th.

8.3.3. Beryllium-7

This naturally occurring radionuclide has a half-life of 53.29 d thereafter decaying to ^{7}Li by electron capture and it is a cosmogenic product of various high energy spallation reactions between cosmic ray neutrons and nitrogen in the atmosphere *ca* 1.5 km above the Earth's surface. It forms BeO molecules which diffuse until meeting dust particles to which they adhere, most forming cloud nuclei with their ^{7}Be incorporating into atmospheric precipitation. Once deposited on the terrestrial surface, entry occurs into the geochemical cycle of beryllium. Although it has a low rate of production, it is an easy cosmogenic radionuclide to detect since it is found practically carrier-free in the atmosphere. Forty years ago, it was suggested that ^{7}Be might be useful in dating and its rapid decay facilitates examining various atmospheric processes, surface water in the oceans and the mixing of sediment in offshore marine and lake environments. Also, some suggested that it could be employed to determine the rate of subsidence of the atmosphere.

8.3.4. Beryllium-10

^{10}Be, with ^{7}Be, is a spallation product cosmic ray-induced in the atmosphere and descends in precipitation to reach sea bottom sediments and continental ice sheets. Its $T_{1/2}$ = 1.5×10^{6} a and its global production rate has been estimated as between 1.5×10^{-2} and 3×10^{-2} atoms $cm^{-2}s^{-1}$, although a lower value has been obtained from Antarctic snow. Like ^{26}Al, it and ^{7}Be are introduced into seas in ionic form and mix with the stable isotopes ^{9}Be and ^{27}Al. Having high ionic potentials, they may become adsorbed on organic and inorganic particles. Sea water has very low concentrations of ^{10}Be compared with river waters and lower concentrations at the surface than in deep water. The residence time has been calculated as *ca* 1,600 a so it is useful for dating authigenic minerals which take it up from ionic solution in the oceans. But there are difficulties because it has a low level of activity and its disintegration rate varies sporadically with depth in cores (associated abundances depending not just on the time elapsed since deposition, but on the rate of deposition and secular variations in production rates too). And clearly it is unwise to assume that the rates of sedimentation in oceans at any particular place were constant for geologically significant time intervals of ~Ma. As well as sediment dating in oceans, ^{10}Be concentrations on land, e.g. in soils, can be examined. However, few data are available due to the low activities encountered. ^{10}Be gave a rate of growth for the manganese nodule measured using ^{26}Al and alluded to above of 2.8±0.06 mm Ma^{-1}. Tektites of various origins were analyzed and some concluded that the radioisotope arose from sediments on the Earth's surface [7]. It is noteworthy that a pair of older tektites (moldavites) *ca* 15 Ma of age had a content less than 0.02×10^{8} atoms of ^{10}Be g^{-1} which may imply that decay took place after their formation as a result of meteoritic impact on the Earth which would confirm their terrestrial origin.

8.3.5. Chlorine-36

This nuclide is cosmic ray-produced in the atmosphere through the nuclear reaction ^{36}Ar(n,p)^{36}Cl, mostly in the stratosphere and its formation is latitude-dependent because of the effect of terrestrial magnetism on cosmic ray intensities. Mixing there is rapid and the concentration of the radioisotope uniform. Its atoms attach to atmospheric aerosols in the sub-micron range which are progressively removed by precipitation from the lower troposphere. Entry from the stratosphere into the troposphere varies seasonally and the fallout rate is greater in middle latitudes than either at the poles or equatorially. This has been given for Stripa in Sweden at 57 °N latitude as *ca* 14±3 atoms m^{-2} s^{-1} [8]. Its $T_{1/2}$ = 0.301×10^{6} a making it valuable for dating glacial ice, exposed volcanics, groundwater, etc. Neutron irradiation of oceanic aerosols following thermonuclear testing at low altitudes induced increased fallout through the nuclear reaction ^{35}Cl(n,γ)^{36}Cl, an effect rising from 1953 to a 1964 maximum of 70,000 atoms m^{-2} s^{-1} [9]. Because such tests were begun earlier over oceans, the ^{36}Cl bomb peak pre-dated that of tritium by *ca* 10 a. A residence time in the atmosphere for Cl^{-} was given as less than 3 years which may be why the bomb pulse of ^{36}Cl was transient with fallout rates dropping back to normal by the early 1970s when low altitude tests were terminated [10]. This bomb pulse was used to study the migration of water through the unsaturated zone into groundwater aquifers and also the stratification of waters in unconfined aquifers. An equation was presented for calculating the ^{36}Cl content (assuming that average fallout is incorporated into the total annual precipitation and that allowance is made for concentration following evapotranspiration [11]. This is:

$$^{36}\mathrm{Cl} = \frac{F\times3.156\times10^{7}}{P}\cdot\frac{100}{100-E}\ \text{atoms litre}^{-1} \qquad (8.3.1)$$

where F is the fallout rate (atoms m^{-2} s^{-1}), P is the mean annual precipitation in mm s^{-1} and E is the evapotranspiration (%).

There is subterranean production of ^{36}Cl and world average chlorine contents of granite and basalt are *ca* 50 ppm and 200 ppm, respectively. Sedimentary rocks have variable contents ranging from *ca* 10 ppm in sandstones to 20,000 ppm in deep sea limestones. Rock outcrops are exposed to the cosmic neutron flux so that some ^{36}Cl results from neutron capture by ^{35}Cl, but below a few meters it is ineffectual. Nevertheless, some ^{36}Cl results from an in situ neutron flux in rock

matrices caused by (α,n) reactions triggered by alpha-particles from U and Th decay systems. This flux was recorded as being of the order of 10^{-4} cm^{-2} s^{-1} by a number of researchers [12].

At Stripa, attempts were made to use data to obtain generalized groundwater regimes. Three were presented as A, B and C. **A** showed groundwater evolution in a granite where salinity is due to interaction with the rock matrix, the ^{36}Cl/Cl atomic ratio of the dissolved chloride characterizing the rock. **B** had the groundwater recharging a formation with lower content of radionuclides (thus lower neutron flux) than the granite so that a lower ^{36}Cl/Cl atomic ratio resulted as chlorinity rose. If chlorinity evolution stopped before this groundwater reached the granite, the ratio would increase with increasing residence time in the granite and the length of this could be estimated from the extra ^{36}C1 in-growth in the granite. **C** assumed chlorinity to derive from a source with a low ^{36}Cl/Cl ratio (possibly an evaporite). Later infiltration into a formation with higher content of radionuclides will produce ^{36}Cl in-growth in the dissolved chloride and if the groundwater resides long enough then the chloride will reach the saturation ratio for the in situ neutron flux. Subsequent flow into a granite fracture system would induce a further time-dependent rise in the ^{36}Cl/Cl atomic ratio if no additional matrix chloride is dissolved. ^{36}Cl deposits in snow on the Greenland ice sheets and in Antarctica and can be used to date ice or detect variations in production rates in the atmosphere.

Another approach to dating ice is based on the ratio ^{36}Cl/^{10}Be, thus:

$$\frac{^{36}\mathrm{Cl}}{^{10}\mathrm{Be}} = \left[\frac{^{36}\mathrm{Cl}}{^{10}\mathrm{Be}}\right]_i e^{-\lambda' t}$$

where λ' is the difference between the decay constants of ^{36}Cl and ^{10}Be.

8.3.6. Krypton-81 and krypton-85

^{81}Kr resembles both ^{39}Ar and the short-lived ^{37}Ar in that it is a cosmogenic radionuclide occurring in the atmosphere, in groundwater which has been in contact with the atmosphere and in occluded air in glacial ice. Both ^{81}Kr and ^{85}Kr result from spallation reactions involving protons and from (n,γ) reactions from the stable ^{80}Kr and ^{84}Kr. ^{81}Kr has a half-life of 2.13×10^5 a and undergoes radioactive decay by EC to the stable nuclide ^{81}Br. It is not a fission product and has an activity of 0.067±0.003 dpm litre^{-1}, a value exceeding expectations by a factor of up to 2 which may imply an extra-terrestrial influence of some sort [13]. ^{85}Kr has $T_{1/2}$ = 10.6 a and decays to the stable nuclide ^{85}Rb by beta emission. It is produced by cosmic ray-related neutrons and also by nuclear fission. The specific activity of anthropogenic. ^{85}Kr was reported as *ca* 3×10^4 dpm litre^{-1} [14]. ^{81}Kr has been used to date glacial ice.

8.3.7. Silicon-32

This is produced by the cosmic ray spallation of Ar in the upper atmosphere from whence it descends to mix with surface water so that, as a radiotracer, it may be applied to measuring ocean water mixing and currents, glacier formation, the accumulation of sediments and the stability of groundwater over centuries. However, its half-life is uncertain, estimates ranging from 60 to 700 a or more; a fairly recent value published in 1986 was 172±4 a [14]. This constrains its utility and another disadvantage is that its extremely low concentrations in planetary waters necessitates utilizing relatively enormous samples (*ca* 10 tonnes of water) for analytical purposes.

8.4. ELECTRON SPIN RESONANCE (ESR)

When dielectric (paramagnetic) solids encounter ionizing radiation, metastable electrons occur and are detectable. Their measurement is feasible using ESR spectrometers able to sense the adsorbtion of microwave radiation by the trapped electrons when they are subjected to a strong magnetic field. This promotes the splitting of the energies of unpaired electrons and how this occurs depends on whether their magnetic moments are aligned parallel to or in opposition to the applied field. ESR-dating is based on such measurements of unpaired electrons trapped in crystal

defects. Such quasi-"free" electrons are produced through geological time by natural radiation arising from the decay of radioactive atoms and also from cosmic radiation. Paramagnetic centres in crystals revealed by ESR are used for dating samples of human and animal bones, fossil shells, corals, stalactites, quartz grains in fault gauges, etc, in the Quaternary era. Hitherto it was believed that the time constraint is due to the short mean life of such paramagnetic centres. However, it has been shown that such defects in quartz may have lasted for at least 1.5 Ga and, since quartz is the most abundant mineral in the Earth's crust, this may have laid the foundation for a greatly extended ESR geochronometer which could be used to date numerous types of geological features over practically the last third of the history of the Earth [15]. But some matters still have to be resolved. The relevant centres can be attributed to Schottky-Frenkel defects in the crystal lattice of quartz and measuring their number is difficult because of the fact that the characteristic ESR lines are frequently small and close to the background signal. Extreme spectrum accumulation has been proposed as a remedy. Then the defects were created by elastic collisions of recoiling α-emitting nuclei with silicon and oxygen atoms and the precise amounts of α-particle emitting nuclides have to be determined. They belong to the U and Th decay chains, but normally have concentrations in quartz in the ppb range which makes them hard to assess. In addition, the number of centres per unit of radioactive nuclides can vary as a function of the type of quartz examined.

8.5. FISSION TRACK DATING (FTD)

When charged particles pass through solids, they lose energy to its atoms and leave damage trails which can be enlarged and made visible optically by chemical etching. Such tracks have dimensions *ca* 10 μm and are created by fission fragments of U. These have been found in natural samples of mica due to the spontaneous fission of ^{238}U and their densities can be used to date e.g. biotite and muscovite (which can contain area densities up to 5,000 cm^{-2}). Their actual numbers reflect the time interval during which they accumulated and the U concentration in the samples. Any selected sample must have enough U content to produce a track density greater than 10 tracks per cm^2 during the time interval from cooling of the sample until now. And the tracks must be stable at ordinary temperatures for periods of time comparable with the age being measured. Tracks can be created also by induced fission of ^{235}U through irradiation of a sample using thermal neutrons in a nuclear reactor, this procedure being termed the "zeta" method of calibrating FTD against other radiometric techniques [16]. Clearly, fission tracks must be reasonably free of defects and lattice ruptures so that they may be counted after etching and the distribution of U in a sample must be close to uniform in order to permit the concentration to be determined from the density of induced tracks. Chemical weathering is adverse to fission tracks and reduces the assessed date of apatite while having little or no effect on zircon or sphene. However, the apparent reduction in date might have resulted from difficulty in identifying tracks in corroded crystals and perhaps also because they may have partially faded through groundwater action. As regards the relevant age equation, most tracks are due to the spontaneous fission of ^{238}U so that the effects of ^{235}U and ^{232}Th can be neglected, also those due to decay by spontaneous fission of naturally occurring radionuclides of high atomic numbers. And induced ^{235}U fission resulting from the adsorbtion of thermal neutrons arising from the spontaneous fission of ^{238}U is insignificant unless the mineral being dated was embedded in uranium ore. The radioactive decay constant for the spontaneous fission of ^{238}U, λ_f, is uncertain, but could be $8.46\pm0.06\times10^{-17}$ a^{-1}. With the usual assumptions, a dating equation is:

$$t = 6.446\times10^{9}\ln\left[1+7.715\times10^{-18}\frac{\rho_s}{\rho_i}\Phi\right] \qquad (8.5.1)$$

where ρ_s is the area density of spontaneous fission tracks on a surface of the mineral being analyzed and ρ_i is the area density of the induced tracks. The time t can be derived after measurement of ρ_s/ρ_i and the relevant neutron dose from the monitor, Φ. Zeta calibration became necessary because of systematic errors arising from uncertainty regarding the value of λ_f which affects FT dates. Parameters of dubious magnitude can be combined into the single calibration factor Z where $Z = \Phi\sigma I/\lambda_f$, σ being the cross-section for the induced fission of ^{235}U by the thermal

neutrons and I the atomic ratio of $^{235}U/^{238}U$. The age equation for a sample of unknown age then becomes:

$$t_{unknown} = \frac{1}{\lambda_a} \ln \left[1 + \frac{\rho_s}{\rho_i}_{unknown} \right] Z\lambda_a \qquad (8.5.2)$$

where λ_a is the decay constant of ^{238}U for α-emission (1.55125×10^{-10} a^{-1}). The value of Z can be obtained by irradiating a mineral sample of known age with every batch of unknown samples. Later, Z is calculated from the measured ratio of the spontaneous and induced track densities of the standard which may be a zircon. The approach has been extended to other minerals too, e.g. apatite and sphene and values for all three in terms of NBS SRM 612 and recorded overall weighted mean zeta (OWMZ) given as 381.8±10.3 for zircon, 353.5±7.8 for apatite and 320±12.4 for sphene, respectively.

Fading of fission tracks when temperatures rise or the mineral is subjected to prolonged heating is represented by the following expression: $t = Ae^{U/kT}$, where t is the annealing time for a specific reduction in fission track density, A is a constant, U is the activation energy in eV, k is Boltzmann's constant and T is the absolute temperature in K. From this, $\ln t = \ln A + U/kT$ and this is the equation of a straight line in coordinates of $\ln t$ and $1/T$ with a positive slope of U/k and an intercept on the y-axis of $\ln A$. Fission tracks fade at different rates. Apatite is a valuable indicator of the cooling history of a rock because of its property of retaining fission tracks only at temperatures appreciably below the blocking temperatures of the Rb/Sr or K/Ar geochronometers in co-existing micas, the precise temperature at which all such tracks are retained depending on the actual cooling rate. FTD can be used in conjunction with estimated geothermal gradients to give information regarding rates of uplift and erosion, e.g. an average uplift rate of 800 m Ma^{-1} over the last 0.5 Ma has been suggested for Nanga Parbat [18]. A recurrent problem in geochronology is how to interpret apparent ages which may represent a mixture of an original formation age with a partial overprint due to a later thermal event. This is because a similar pattern may arise from slow cooling from the original age of formation. However, below *ca* 350 °C (the only range where FTD is applicable), overprinted and slow cooling models can sometimes be distinguished. Spontaneous fission tracks have a relatively constant initial length which reflects energy freed in the fission decay and also the nature of the recording medium. They shorten progressively in the course of thermal annealing. But each track is different in age from the others and so underwent a different fraction of the total thermal history of the mineral sample. Hence, in a U-bearing mineral with a complex thermal history, the lengths of the different groups of fission tracks will vary according to when the members formed and thus the track distribution plus the apparent fission age facilitate reconstructing the variation of temperature through geological time. Australian data from samples of apatite obtained from deep drill holes where temperatures are now within the annealing zone for this mineral showed that, at subsurface temperatures of *ca* 100 °C and above, the length distributions became very broad with no pronounced peak. Longest track lengths stayed more or less constant and it was concluded that confined track lengths indicate thermal history in the temperature zone of increasing track stability. The reported length distributions gave a basis for interpreting fission track ages [19]. An apatite age caused by a uniform slow cooling thermal history showed a broad, negatively-skewed, length distribution while a bimodal distribution evidenced a two-stage thermal history entailing partial annealing by a discrete thermal event.

8.6. IODINE/XENON

In total, iodine has 33 isotopes of which 16 are radioactive. The one of interest is ^{129}I (half-life = 15.7×10^6 a). Common iodine is ^{127}I (relative abundance 100%). Xenon is an inert (noble) gas, and it is present in the atmosphere in minute amounts (*ca* 0.006 ppm). Xenon has 36 isotopes of which ^{129}Xe is the one of interest. It has an abundance in the naturally occurring element of 26.4 atom %. The I-Xe system is based on the radioactive decay of 15.7 Ma ^{129}I and could be a potentially precise geochronometer, especially of early events in the Solar System. Lack of knowledge as to how it responded to thermal events during the post-formation histories of ordinary chondritic meteorites restricts its applicability.

8.7. LUTETIUM/HAFNIUM

8.7.1. Methodology

This depends on the beta decay of a naturally occurring radionuclide and, as with Re/Os and K/Ca, Lu/Hf dating is applicable to minerals and rocks which cannot be investigated by other conventional methods. ^{176}Lu undergoes branched decay mostly to ^{176}Hf, but *ca* 3±1% decays to ^{176}Yb. The scheme of interest is $^{176}\text{Lu} \rightarrow {}^{176}\text{Hf} + \beta^- + \bar{\nu} + Q$ which leads to an excited state of ^{176}Hf succeeded by γ-emission. Attempts have been to obtain the half-life of ^{176}Lu and various results have been presented, these ranging from 2×10^{10} a to 7×10^{10} a. One figure was calculated from the slope of a Lu/Hf isochron formed by 10 achondrites (eucrites) with an age of 4.55 Ga and this was 3.53×10^{10} a with a corresponding decay constant of $1.96\pm0.08\times10^{-11}$ a^{-1} later revised to $1.94\pm0.07\times10^{-11}$ a^{-1} [20]. Lu and Hf occur in most rocks and the most important lutetium-bearing minerals are zircon, biotite and apatite together with some rare earth element ones such as the phosphates monazite and xenotime. Because Hf can replace zirconium, it occurs most commonly in zircon.

8.7.2. Assessment of ages

Because of the radioactive decay of ^{176}Lu, the abundance of ^{176}Hf in lutetium-bearing rocks increases with time. The age is obtainable by solving an equation of the following type:

$$\frac{^{176}\text{Hf}}{^{177}\text{Hf}} = \left[\frac{^{176}\text{Hf}}{^{177}\text{Hf}}\right]_i + \frac{^{176}\text{Lu}}{^{177}\text{Hf}}\left(e^{-\lambda t} - 1\right) \qquad (8.7.1)$$

where the first term refers to the relevant ratio in present day samples, the second refers to the initial ratio which obtained when the system formed and the third refers to the Lu/Hf ratio at present, λ being the decay constant of ^{176}Lu. To determine the age of a mineral containing Lu and Hf, therefore, it is necessary to measure concentrations of these elements and also the ^{176}Hf/^{177}Hf ratio. The equation can be solved for t if the initial value of this ratio is known accurately, the decay constant is known accurately and the system has remained closed to both elements during its geological history.

8.7.3. Isochrons

If a suite of samples has a common age, but differing Lu/Hf ratios with the same initial $[^{176}\text{Hf}/^{177}\text{Hf}]_i$ ratio, all will lie on a straight line isochron in coordinates of ^{176}Hf/^{177}Hf, its slope being proportional to their age and its intercept being the initial $[^{176}\text{Hf}/^{177}\text{Hf}]_i$ ratio. Data were published on suite of total rock samples and separated zircons from the Amitsoq gneiss, West Greenland and the relevant isochron gave an age of 3.59±0.22 Ga and an initial $[^{176}\text{Hf}/^{177}\text{Hf}]_i$ ratio of 0.280482±0.000033 [21]. This agreed well with those obtained using the Rb/Sr method and quite well with U, Th, Pb dating too. Hence this date is perhaps a reasonable estimate of the time elapsed since the sources of the Amitsoq gneiss were transferred up from the mantle.

8.7.4. Hafnium through time

From the chondrite meteorite Murchison, the Lu/Hf ratio was stated to be 0.24 and, assuming that the age of a chondritic reservoir is 4.55 Ga, the present value of the ^{176}Hf/^{177}Hf should be 0.28286, taking into account the corresponding ^{176}Lu/^{177}Hf ratio of this chondrite which is 0.0334.

These data define a Hf growth curve useful as a reference for the isotopic composition of Hf in terrestrial rocks and minerals. The relationship may be expressed by an ε-parameter thus:

$$\varepsilon^{o}(\text{Hf}) = \left[\frac{\left(^{176}\text{Hf}/^{177}\text{Hf}\right)_{sa}}{\left(^{176}\text{Hf}/^{177}\text{Hf}\right)_{ch}} - 1\right]\times10^4, \text{ sa = sample, ch = chondrite,}$$

and this notation of ε^{o}(Hf) shows that the present Hf isotope ratios are being compared. The parameter ε^{i}(Hf) refers to a comparison in the past based on initial $^{176}Hf/^{177}Hf$ ratios and is stated below:

$$\varepsilon^{i}(Hf)=\left[\frac{\left(^{176}Hf/^{177}Hf\right)^{i}_{sa}}{\left(^{176}Hf/^{177}Hf\right)^{t}_{ch}}-1\right]\times 10^{4}$$

where $(^{176}Hf/^{177}Hf)_{sa}$ is the initial value in a sample corrected for decay after it formed and $(^{176}Hf/^{177}Hf)_{ch}$ is the value in the chondrite reservoir *t*/a years ago. This latter can be calculated from the following:

$$\left[\frac{^{176}Hf}{^{176}Hf}\right]^{t}_{ch}=0.28286-0.334(e^{-\lambda t}-1)$$

where *t* is the time elapsed since the sample formed. Positive ε means that the sample is enriched in radiogenic ^{176}Hf compared with the chondritic reservoir and therefore probably originated from a source with a higher Lu/Hf ratio than the chondrites. On the other hand, negative ε values result from a deficiency of ^{176}Hf and the relevant samples may have come from a source with a lower Lu/Hf ratio than the chondrite reservoir. In basalts from mid-oceanic ridges (MORB) and oceanic islands (OIB), the $^{176}Hf/^{177}Hf$ ratios range from 0.2828 to 0.2835 and usually exceed the present ratio in the chondritic reservoir. Such basalts may have been derived from sources in the mantle which became depleted in Hf relative to Lu during earlier episodes of partial melting. Hence, they have higher Lu/Hf ratios than chondrites. Interestingly the $^{176}Hf/^{177}Hf$ ratios of oceanic basalts correlate negatively with $^{87}Sr/^{86}Sr$ ratios and positively with $^{143}Nd/^{144}Nd$ ratios according to some researchers [22]. Hf/Sr and Hf/Nd isotope mantle arrays have been divided into quadrants using the proposed isotope ratios of the chondritic reservoir which follow: $^{176}Hf/^{177}Hf = 0.28286$, $^{87}Sr/^{86}Sr = 0.7045$, $^{143}Nd/^{144}Nd = 0.512638$. The geochemical histories of the magma sources of the igneous rocks found in these quadrants have been expressed using a fractionation factor *f* thus:

$$f_{Lu}=\left[\frac{^{176}Lu/^{177}Hf}{\left(^{176}Lu/^{177}Hf\right)^{o}_{ch}}\right]-1$$

where $^{176}Lu/^{177}Hf$ is the value of this ratio in a rock or magma source now and the chondritic reservoir has $(^{176}Hf/^{177}Hf)_{ch} = 0.3334$. It is clear that sources enriched in Lu and depleted in Hf will have $f_{Lu}>0$ and vice versa. The range of $^{176}Hf/^{177}Hf$ ratios in MORBs has been quoted as 0.283112 to 0.283476 which places them in quadrants characterised by $f_{Lu}=>0$. This range implies that the mean time-integrated Lu/Hf ratios of the relevant sources vary from 0.251 to 0.279. The chondrite reservoir is thought to have a Lu/Hf ratio of 0.24, therefore these sources must have been enriched in Lu before more MORB magmas formed, perhaps soon after the Earth formed. And, as MORBs contain at least 11.8 times more Lu and 14.4 times more Hf than chondrites, it may be inferred that, even though both elements are strongly partitioned into the silicate liquid, Hf is concentrated more than Lu.

8.8. OSMIUM/OSMIUM

8.8.1. Methodology

Since N-TIMS (negative thermal ion mass spectrometry) for Re/Os was developed *ca* 1990, only a few publications showing its wide applicability have appeared. This is mainly due to the high Re blank from the current generation of "clean" Pt filaments and to problems in achieving isotopic exchange and equilibrium between sample and spike for Os. Also inhomogeneity of samples is a serious drawback. Due to this, Re and Os concentrations may vary by up to 40% in the same sample. However, avoiding or overcoming these difficulties may be possible using "Os/Os" ($^{187}Os/^{186}Os$ and $^{187}Os/^{188}Os$) dating [23]. This is a high precision approach and its use with a molybdenite sample implied that it can become a geochronological tool even capable of dating minerals from meteorites. Irradiating a rhenium-bearing sample with thermal neutrons in a nuclear reactor produces enrichment of ^{186}Os and ^{188}Os in proportion to the neutron fluence and the Re/Os ratio of the relevant sample. After free decay, the quantities of these induced by thermal neutrons (Os*) are given by:

$$^{186}Os^{*}=0.922\ C\ ^{186}Re=0.922\ C\ ^{185}Re\Delta T\int_0^{\infty}(\varepsilon)\sigma_{185}(\varepsilon)d\varepsilon\ ,\ \text{and}$$

$$^{188}Os^{*}=^{188}Re=^{187}Re\ \Delta T\int_0^{\infty}\varphi(\varepsilon)\sigma_{187}(\varepsilon)d\varepsilon$$

where 0.922 is the branching ratio, ΔT is the length of irradiation, φ (ε) is the neutron flux at energy ε. C is introduced because $^{186}Re_{metastable}$ will not reach ^{186} because of its long half-life. The above is reminiscent of the $^{40}Ar/^{39}Ar$ method. The half-lives of $^{186}Re_{ground\ state}$ and ^{188}Re are 90.6 h and 16.7 h, respectively. The former undergoes the branched decay, 92.2% β-decaying to stable ^{186}Os and 7.8% decaying by EC to stable ^{186}W. Ages can be calculated, if neutron fluxes and cross sections are known, from the following:

$$t_{186}=\frac{1}{\lambda_{187}}\ln\left[\frac{\left(\frac{^{187}Os}{^{192}Os}\right)_s-\left(\frac{^{187}Os}{^{192}Os}\right)_i}{\left(\frac{^{186}Os}{^{192}Os}\right)_s-\left(\frac{^{186}Os}{^{192}Os}\right)_n}\frac{^{185}Re}{^{187}Re}0.922\ C\ F_{185}+1\right],$$

$$t_{188}=\frac{1}{\lambda_{187}}\ln\left[\frac{\left(\frac{^{187}Os}{^{192}Os}\right)_s-\left(\frac{^{187}Os}{^{192}Os}\right)_i}{\left(\frac{^{188}Os}{^{192}Os}\right)_s-\left(\frac{^{188}Os}{^{192}Os}\right)_n}F_{187}+1\right]$$

where s = measured ratios, n = normal ratios, i = initial ratios of samples and F is a fluence term. These parameters are difficult to evaluate for various reasons and the influence of interfering reactions must be estimated as well. The $T_{1/2}$ of ^{187}Re is not known precisely, but probably lies at *ca* 4.27×10^{10} a with $\lambda=1.64\pm0.05\times10^{-11}\ a^{-1}$. If just the isotopic composition of a sample is analyzed, 2 ages are obtained and should be consistent. In an irradiated sample of molybdenite, the measured $^{186}Os/^{192}Os$ was 0.3284 and the measured $^{188}Os/^{192}Os$ was 0.6299 (and these are assumed to be 0.0390 and 0.3248 in an unirradiated sample). The ratios could be measured using N-TIMS to a precision of 1%. Derived ages came out as $t_{186}=220.5\pm8.7$ Ma and $t_{188}=214.9\pm 8.9$ Ma, respectively, or ±1.4 Ma and ±1.7 Ma, respectively, when the uncertainty of the ^{187}Re half-life is excluded). These values agreed with 221 Ma to 238 Ma K/Ar ages of the leucogranite emplacement causing the Mo mineralization at the relevant site (Kingsgate molybdenum mine,

New South Wales, Australia). But while errors connected with the irradiation parameters can be considerably reduced by choosing a suitable neutron flux monitor, a constraint is still exerted by the uncertainty in the $T_{1/2}$ of ^{187}Re.

Os/Os dating eliminates experimental problems characterising conventional Re/Os analyses and enables both the Re/Os ratio and the Os isotopic composition to be obtained from a single isotopic-measurement. Clearly, the precision of age determinations will reflect the instrumental precision of Os isotope ratio measurements using N-TIMS. The method would seem to offer possibilities of dating open systems, that is to say obtaining age spectra by selective leaching or by in situ measurement of irradiated samples. However, the analytical procedures must be further refined, particularly as regards the flux monitor. Obviously establishing and certifying an appropriate monitor would facilitate extending the Os/Os method. And, since ^{186}Os, ^{187}Os and ^{188}Os are variable and for ^{189}Os there is significant ^{18}O interference, e.g. in molybdenites, only $^{190}Os/^{192}Os$ can be utilized for the fractionation correction in all Os/Os dating measurements. MPI-Os is an available standard.

8.9. POLONIUM/LEAD

The isotopes of lead are discussed in the chapter on uranium/thorium/lead dating.

Polonium is a radioactive element with twenty-seven isotopes of which the longest-lived has a mass number of 209 and a half-life of 103 a. The isotope of interest in this new geochronometer, first presented by Rubin et al [23b], is ^{210}Po which occurs in some uranium ores to an extent of about 1 part in 10^{10} parts (mass of Po to mass of U). Its half-life is 138.4 d and it is a member of the ^{238}U decay series. It has the same activity as all other nuclides in this series in an undisturbed system, that is to say one at secular or radioactive equilibrium. Polonium is moderately volatile and hence gaseous at 400 °C in volcanic emissions. It is possible that polonium volatilizes as a halogen-containing species and it appears to be completely de-gassed in freshly erupted sub-aerial lavas at various volcanic sites such as Kilauea and Etna. In these, its activity shifts towards equilibrium with the parents in the decay series following the half-life, the immediate one being ^{210}Bi (half-life 5.013 d). After a fractionation event, this latter rapidly equilibrates with its parent which is ^{210}Pb. The sequence is illustrated in Figure 8.20.1 (Uranium-Radium $A = 4n + 2$) in the chapter on uranium/thorium/lead dating elsewhere in this book. Therefore, the rate of change of ^{210}Po in such newly erupted lavas is effectively controlled by ^{210}Pb decay within half an hour or so of the events taking place. Unlike ^{210}Po, almost no Pb de-gasses during them so that the de-gassing of ^{210}Po sets the geochronometer for volcanic rocks at such periods and the times since occurrence can be assessed using the degree of ingrowth to equilibrium with ^{210}Pb.

8.9.1. Methodology

Rubin et al [23b] used a simplified form of the Bateman equation for closed-system decay to describe the ^{210}Po content of de-gassed lavas as a function of time thus:

$$\left(^{210}Po\right)_t = \left(^{210}Po\right)_{t=0}\left[e^{-\lambda t}\right] + \left(^{210}Pb\right)\left[1 - e^{-\lambda t}\right]$$

where t is the time elapsed since the eruption and λ is the decay constant. Parentheses are utilized to show activities. It is clear that, to calculate t from a single measurement of (^{210}Po) it would be necessary to know both (^{210}Pb) and $(^{210}Po)_{t=0}$. While, for a totally de-gassed lava, the latter term would be zero, it is probable that only partial de-gassing may occur in the case of submarine lavas which erupted under high hydrostatic pressures. However, it is feasible to calculate a unique maximum value for t by assuming that total de-gassing took place and fitting an exponential function to a set of measurements made on a sample as ^{210}Po grows into equilibrium with ^{210}Pb. The maximum age corresponds with $(^{210}Po)=0$ on the best-fit ingrowth curve. Rubin et al [23b] applied the approach to East Pacific Rise (EPR) lavas and made repeat measurements of (^{210}Po) over several years on aliquots of each sample together with ingrowth curves having the functional form of the above equation, fitting these to the data using the time interval between sequential measurements in order to constrain t. The regression results gave a function for (^{210}Po) and the known analysis times linked the results to calendar time.

If Po de-gassing was not total at eruption, the eruption time cannot be precisely ascertained, but is bracketed in every instance by the "window" between collection of sample and calculated maximum age. Such "windows" (eruption dates) are most accurately determinable for samples either having the lowest (^{210}Po) when collected or for which the initial (^{210}Po) can be estimated independently.

Samples came from mid-ocean ridge basalts (MORBs) and these have similar chemical compositions and were erupted at the same water depth, both of these factors perhaps affecting the efficiency of de-gassing. Thus it can be anticipated that that all will have had more or less the same initial (^{210}Po). But the de-gassing content may not be as high as the sub-aerial value of 100%. Two of the samples analyzed by Rubin et al [23b] had ^{210}Pb contents at the time of collection which were only *ca* 25% of the secular equilibrium value (25.1% and 25.6%, respectively) which implies that all samples were minimally 75% de-gassed in the course of eruption.

Best-estimate eruption "windows" are *ca* 2 months long and permit investigation of MORB eruption chronology on a far finer scale than hitherto possible. If Po de-gassing turns out usually to be larger than Rubin et al's "conservative" minimum estimate of 75%, then the resolution of the technique may improve, although such bettering would necessitate analyses of ^{210}Po in a number of very young MORBs having eruption dates which are well known so that the normal degree of de-gassing could be established. These authors proposed that making remote observations of potential eruption indicators falling within an eruption "window", e.g. seismicity or megaplumes, could be additionally valuable in constraining eruption dates and the range of initial ^{210}Po in MORBs. Some of their eruption "windows" were uncertain because they were not able to make more than two ^{210}Po analyses on each of the relevant lavas. Nevertheless, the results demonstrated that they are younger than the eruptions of early 1991 and must have erupted between the 1991 and 1982 expeditions. Consequently the Rubin et al [23b] ^{210}Po/^{210}Pb dating work explicitly showed that a small part of the EPR underwent eruptions during the first few months of 1991 and again during late 1991/early 1992. Clearly, such information is invaluable for evaluating the frequency and volume of eruptions within an eruptive cycle as well as short-term variations in MORB chemistry in a small area. Also, it can shed light on such matters as whether changes in lava chemistry relate to hydrothermal vent fluid chemistry and how rapidly biological communities respond to eruption-induced environmental changes.

All of the lavas with ^{210}Po eruption "windows" in the early months of 1991 are mafic (>8.5% wt% MgO) MORB with almost the same chemical composition. Rubin et al [23b] regarded the Po data as being consistent with them being separate samples of one single flow only if the degree of de-gassing was very variable when eruption occurred, actually from total to 75%. In addition, although all were collected close to each other, at least one came from a physically different flow unit. From this, they inferred that the relevant samples originated from a number of separate flows arising from a homogeneous magma reservoir through about four months, but comprising one volcanic episode. Two younger lavas were distinguishable from the above set and had distinct eruption "windows" which was taken as evidence of origin as separate events either stemming from a different magma reservoir or having an intervening alteration in the lava composition. One of these younger lava samples was collected from the same area as the 1991 flows and was practically chemically identical to them. The implication was that the magma reservoir contributing lavas to what Rubin et al.[23b] termed the "tubeworm barbecue" site retained an essentially constant chemical composition over a time interval of one year or more. However, one sample was obtained approximately 5 km to the north so that it remained unclear whether its different chemical composition is temporal or spatial in nature. The younger age of the flow accords with other observations suggesting that volcanicity shifted northwards into a previously inactive region. That Po, de-gasses from erupting mid-oceanic ridge lavas intimates the operating of similar mechanisms involving other volatile and f'airly volatile metals and, if true, estimates of their fluxes into seawater based solely upon information from mid-oceanic ridge hydrothermal systems would be lower limits. Of course, the de-gassing process may well affect just the surfaces of flow since Po in the one microcrystalline sample analyzed by Rubin et al [23b] was <20% de-gassed on eruption. It is apparent that further work aimed at evaluating fine-scale variations in Po and other volatiles, e.g. carbon dioxide and volatile metals, with depth in submarine flows is mandatory.

Rubin et al.[23b] regarded the significance of their work on ^{210}Po/^{210}Pb dating as two-fold, namely it confirmed suspicions of mid-oceanic ridge eruptions shortly prior to the April 1991 visit

to 9°50' N on the EPR of the submersible "Alvin" and also produced the only information regarding both the number and timing of these phenomena. Revisiting the area after a nine months lapse revealed that a lot of the physical evidence for recent volcanic activity had disappeared, although other adjacent regions seemed to be active. It is clear that the $^{210}Po/^{210}Pb$ chronometer potentially can provide data apropos the temporal variability of such submarine eruptions with excellent time resolution, especially when utilized together with detailed direct and remote observations. Rubin et al [23b] concluded that this chronometer, in conjunction with other radioactive tracers of MORB eruptions, may well improve understanding the temporal variability of submarine eruptions and their effects on both the biology and geology of the ridge ecosystem.

8.10. POTASSIUM/ARGON

8.10.1. Methodology

After identification of the naturally occurring radioactive nuclide ^{40}K, it was found that it undergoes branched decay to ^{40}Ar and ^{40}Ca, hence ^{40}Ar abundance in the atmosphere is orders of magnitude greater than would be expected by comparison with abundances of the other noble gases. Thus excess ^{40}Ar should occur in ancient potassium-bearing minerals and, once this was found to be the case, the foundation of the K/Ar dating method was laid. The relative abundances of the 3 significant K isotopes are: ^{39}K 93.2581%, ^{40}K 0.0117% and ^{41}K 6.7302%. Those of the Ar isotopes of interest are: ^{36}Ar 0.337%, ^{38}Ar 0.063% and ^{40}Ar 99.6%. Decay of ^{40}K to stable ^{40}Ar takes place by EC, also by negatron and positron decay with emission of γ-quanta (energy 1.51 MeV). 11% of the ^{40}K decays by EC to an excited state of ^{40}Ar which de-excites by emitting a gamma ray. Ca 0.16% of the decays take a more direct route by e.c. straight to the ground state of ^{40}Ar. Positron decay is rare, occurring only *ca* 0.001% of the time with an E_{max}=0.49 MeV. It is followed by 2 annihilation gamma rays with a combined energy of 1.02 MeV. Decay to stable ^{40}Ca involves most of the ^{40}K atoms and actually only 11% of them decay to ^{40}Ar. In a potassium-bearing system which has been closed to all external influences during geological time, the growth of radiogenic ^{40}Ar and ^{40}Ca may be represented as follows:

$$^{40}Ar + ^{40}Ca = ^{40}K\,(e^{-\lambda t} - 1)$$

where λ is the total decay constant of ^{40}K. Of course, each branch of the decay mode has its own decay constant which are, for ^{40}K to ^{40}Ar 0.581×10^{-10} a^{-1}, and for ^{40}K to ^{40}Ca 4.962×10^{-10} a^{-1}, respectively. Summing these gives a value for λ of 5.543×10^{-10} a^{-1}. The corresponding $T_{1/2}$=1.25 $\times10^{9}$ a. The branching ratio is *ca* 0.11. It must be added that there are other, slightly different, values for the decay constants in the literature. The growth of radiogenic ^{40}Ar atoms in a potassium-bearing mineral is given by:

$$^{40}Ar = \frac{\lambda_{ec}}{\lambda}\,^{40}K\left(e^{\lambda t} - 1\right)$$

where λ_{ec} is the decay constant for the system ^{40}K to ^{40}Ar. The total number of ^{40}Ar atoms will be the sum of the radiogenic ones and any present when the mineral formed. It is assumed that none was present initially and, if this is justifiable, then, if we know the ^{40}K concentration and the amount of accumulated radiogenic ^{40}Ar in a mineral, its age can be obtained from:

$$t = \frac{1}{\lambda}\ln\frac{^{40}Ar}{^{40}K}\left[\frac{\lambda}{\lambda_{ec}}\right] + 1 \qquad (8.10.1)$$

where t is age. Some other assumptions have to be made in order to derive values for t from various minerals. One is that none of the radiogenic ^{40}Ar arising from the radioactive decay of ^{40}K in the mineral during its geological history has escaped by diffusion. Another is that the mineral closed to ^{40}Ar soon after crystallization, hence rapid cooling must have taken place. It is implicit in the method that no excess ^{40}Ar became incorporated in the mineral when it crystallized or during any subsequent metamorphic episodes. Finally, it is assumed that the mineral remained closed to K

throughout its geological history so that the isotopic composition of the K in it must have altered solely through radioactive decay of the ^{40}K originally present and no isotopic fractionation occurred. A correction is necessary for the presence of atmospheric ^{40}Ar. Also, the potentially disturbing effects of Ar being over-pressured in extremely old basement rocks have to be considered because the gas might be released during metamorphism [24]. However, it has been asserted that this may not always happen because analyses of Alpine muscovites in granites from the Helvetic basement (Aar Massif) in the central Swiss Alps showed no Ar over-pressure either of radiogenic or atmospheric origins existed [25].

8.10.2. Argon loss

If this occurred in a mineral, the usual reason is metamorphism and the phenomenon demonstrates the inability of Ar to bond with other atoms in a crystal lattice. In fact, minerals have difficulty in retaining the gas even at quite low temperatures and at atmospheric pressure. Hence, it is not surprising that the concept of closure temperatures (below which, when minerals form, crystallization ages are recorded) has been increasingly criticized. Researches in the western Alps and Norway demonstrated that old ages were retained despite later metamorphic temperatures believed to have exceeded the supposed closure temperatures [26,27]. The inference is other factors may affect mineral age relationships. For instance, chemical weathering, alteration by aqueous fluids, deformation, ex-solution and recrystallization. Obviously only potassium-bearing rocks and minerals able to resist as many as possible of these adverse influences are appropriate for dating by the K/Ar method. Such rocks and minerals are fairly common and, among igneous rocks, include volcanics, although those including de-vitrified glass must be avoided as also should those having such secondary minerals as xenocrysts. Basaltic glass can retain Ar well, but hydrated glass cannot, especially when de-vitrified. De-vitrified glass data showed a lowering of K/Ar dates. Xenocrysts may produce the opposite effect if they possess excess radiogenic ^{40}Ar. Such excess radiogenic ^{40}Ar may be present in some potassium-bearing minerals and its effects on K/Ar ages are most marked in young minerals or those with a low K content. However, while beryl, cordierite and tourmaline often contain such excess radiogenic ^{40}Ar, other minerals do not. The excess gas can result from the relevant minerals undergoing a high partial pressure of the gas during an episode of regional metamorphism when pegmatites crystallize or kimberlite pipes are emplaced. In addition, it may diffuse into minerals as a result of out-gassing of older potassium-bearing ones in the crust and mantle of the Earth or from older xenoliths or xenocrysts. Wherever it occurs, K/Ar ages are increased and hence give over-estimates for the dates of minerals containing it. Minerals used in such dating have different blocking temperatures, e.g. that of biotite is lower than that of hornblende in deep seated plutons and so the K/Ar "clock" of the hornblende starts before that of biotite since cooling is in progress. Clearly, if temperature decrease was smooth and both minerals constituted closed systems since crystallization, the hornblende will register an older date than the biotite. If two such different dates are obtained, they can be used to infer the cooling rate. But discordant K/Ar dates from co-existing minerals have been recorded in metamorphic rock samples from metamorphic rocks having two separate temperature histories. In such cases, either all the minerals were totally de-gassed in the course of the metamorphic episode and slow cooling followed or the de-gassing process did not go to completion and the fraction of Ar lost from a particular mineral will relate to the retentivity of that mineral for the gas. Many biotites from granitic gneisses and schists of Precambrian age shields and orogenic belts have been dated by the method and results often reflected times elapsed after cooling through blocking temperatures rather than real ages of the relevant minerals. If such dates are plotted on a map, they form a conceptual surface termed the metamorphic veil [28]. The meaning of this is that the K/Ar dates veil the real ages of the host rocks and show only the regional metamorphic episode and the later cooling histories of the rocks. Regional homogeneity for such dates in shields and orogens implies that large parts of the continental crust may have undergone metamorphism, later cooling in large scale systematic patterns perhaps being induced by the uplifting of vast cratonic blocks bordered by extensive fracture zones extending far below the surface. Perhaps the K/Ar dates from an individual mineral of such a cratonic block might represent the time interval which elapsed since rocks now exposed at the surface were up-thrust across the isotherm corresponding to the blocking temperature of that mineral. Contours drawn to represent equal times since cooling through blocking temperatures have been called thermochrons or chronochrons. In the Grenville Province,

Canada, they run roughly parallel to the Grenville Front to form a surface dipping southeastwards. Rocks exposed now were uplifted through the blocking temperature isotherm between 850 Ma and 1.125 Ga ago and the western edge of the Grenville cration was uplifted before the eastern edge. However, if the lower dates along the eastern edge are due to argon loss induced thermally during the Appalachian orogeny, this would be an alternative explanation. Data from the Canadian Shield cluster round certain values which may relate to the presumed ages of orogenies of which there were at least 4 of which the time scale was determined by K/Ar, whole rock Rb/Sr and U/Pb dating [29]. In association with this, 8 structural provinces were recognized on the Canadian Shield and each stabilized at the end of a particular orogeny (shown by the clustering of K/Ar mica dates around a "magic number"). But the metamorphic veiling must be remembered – it conceals the real ages so that, e.g. the Grenville Province has rocks formed much earlier than the Grenville orogeny. A similar time scale has been constructed for the USA.

8.10.3. Isochrons

If the equation for growth of radiogenic ^{40}Ar atoms in a potassium-bearing mineral stated earlier is modified by dividing all terms by ^{36}Ar, the following expression is obtained:

$$\frac{^{40}Ar}{^{36}Ar} = \left[\frac{^{40}Ar}{^{36}Ar}\right]_i + \left[\frac{\lambda}{\lambda_{ec}}\right]\left[\frac{^{40}K}{^{36}Ar}\right]\left(e^{-\lambda t} - 1\right)$$

which gives the measured $^{40}Ar/^{36}Ar$ ratio as a sum of 2 terms of which the first refers to the Ar donated by igneous, metamorphic and atmospheric sources and the second refers to the radiogenic component accumulated since closure of the relevant mineral system. Generally this ratio depends on the isotopic composition of the different Ar components and will probably differ from that of atmospheric Ar. However, potassium-bearing minerals co-existing in a rock sample will have similar, if not identical, such ratios and, under these circumstances, the equation represents a set of straight lines in coordinates of $^{40}Ar/^{36}Ar$ and $^{40}K/^{36}Ar$. If compared to that of a straight line in the slope intercept form $y = b + mx$, then the intercept on the y-axis will be given by $b = [^{40}Ar/^{36}Ar]_i$ and the slope will be $m = (\lambda_e/\lambda)(e^{-\lambda t}-1)$. Hence such co-existing minerals with the same presumed initial $[^{40}Ar/^{36}Ar]_i$ ratio and the same age can be represented bypoints defining a straight line in coordinates of the measured $^{40}Ar/^{36}Ar$ and $^{40}K/^{36}Ar$ ratios, this constituting an isochron. The slope of such an isochron, m, can be used to calculate the relevant age as follows:

$$t = \frac{1}{\lambda}\ln\left[m \cdot \frac{\lambda}{\lambda_e} + 1\right] \qquad (8.10.2)$$

where t is the time elapsed since crystallization. Such K/Ar isochrons have been extensively utilized and it is clear that they form only when all the samples involved are closed systems with respect to K and Ar; this ensures that the derived data points define the relevant slopes satisfactorily. The isochron approach is probably more advantageous than conventional K/Ar dating because the degree of good fit of such data points to a straight line expresses the degree of closure of the samples analyzed through geological time as well as the similarity or concordance of their initial $[^{40}Ar/^{36}Ar]_i$ isotopic ratios. As such initial ratios have been found to exceed atmospheric value, it may be inferred that Ar originally incorporated into minerals showing this effect did not come entirely from the atmosphere, but rather included constituents deriving from elsewhere, maybe as a result of the out-gassing of old crustal rocks or even the mantle of the Earth. Ar from such sources is highly enriched in ^{40}Ar relative to ^{36}Ar and such extraneous radiogenic ^{40}Ar yields conventional K/Ar dates of minerals which far exceed the actual ages of the host rocks. If difficulties arise because different potassium-bearing minerals from a given rock sample show different initial $^{40}Ar/^{36}Ar$ ratios through variable atmospheric Ar contamination, this can be minimized or even obviated by either leaching with hydrofluoric acid or pre-heating under vacuum before Ar is extracted. It should be mentioned that some researchers are sceptical about this solution. And spurious K/Ar isochrons may stem from rocks containing minerals with different closure temperatures because the correlation of radiogenic ^{40}Ar and ^{40}K here is due to mixing and the mixture lines which result are of no significance geochronologically.

8.11. POTASSIUM/CALCIUM

Ca has 6 stable isotopes occurring naturally with the following abundances: ^{40}Ca 96.98215, ^{42}Ca 0.6421%, ^{43}Ca 0.1334%, ^{44}Ca 0.20567 ^{46}Ca 0. 0031% and ^{48}Ca 0.1824%. Its isotopic composition in minerals and rocks varies through the formation of ^{40}Ca by the negatron decay of ^{40}K (along one path of branched decay, the other leading to ^{40}Ar) and also because of the fractionation of Ca isotopes during several physico-chemical processes. The possibility of Ca isotopes fractionating is improved by the considerable difference in their masses (ca 20% for ^{48}Ca relative to ^{40}Ca). The decay constant for the system ^{40}K to ^{40}Ca is *ca* 4.962×10^{-10} a^{-1}. The following expression can be applied:

$$\frac{^{40}Ca}{^{42}Ca} = \left[\frac{^{40}Ca}{^{42}Ca}\right]_i + \frac{\lambda_{\beta^-}}{\lambda_{ec}+\lambda_{\beta^-}}\left[\frac{^{40}K}{^{42}Ca}\right]\left(e^{-\lambda t}-1\right)$$

where $\lambda=\lambda_{ec}+\lambda_{\beta-}$ and the first term is the ratio of the relevant isotopes now, the second is the initial ratio when the system formed or was last isotopically homogenized and the λ-values are the appropriate decay constants, $^{40}Ca/^{42}Ca$ being the ratio of the respective isotopes in the mineral sample. Co-genetic rocks or minerals having the same initial $[^{40}C/^{42}Ca]_i$ ratio and of the same age lie on an isochron in coordinates of $^{40}Ca/^{42}Ca$ and $^{40}K/^{42}Ca$ with a slope of $m=\lambda_{\beta-}/\lambda(e^{-\lambda t}-1)$ and an intercept equal to the original $^{40}Ca/^{42}Ca$ ratio. High precision values for the ratio $^{40}Ca/^{42}Ca$ relative to $^{42}Ca/^{44}Ca$ were *ca* 0.31221, a useful reference for making fractionation corrections. The Pikes Peak batholith, Colorado, USA, was dated at 1.041±0.032 Ga by isochron and this agreed closely with results from other isotopic geochronometers [30]. The initial $[^{40}Ca/^{42}Ca]_i$ ratio was 151.024±0.016. This is almost the same as that obtained from 2 stony meteorites and 3 mantle-derived rocks and minerals. The mantle level was so low that it implied preservation of the primordial isotopic composition of Ca. Differences in the isotopic composition of Ca caused by ^{40}K decay or isotopic fractionation can be expressed by an ε-parameter:

$$\varepsilon_{Ca} = \left[\frac{\left(^{40}Ca/^{42}Ca\right)spi}{\left(^{40}Ca/^{42}Ca\right)mantle} - 1\right]\times 10^4$$

where the $^{40}Ca/^{42}Ca$ ratio of the mantle is 151.016±0.011. At Pikes Peak, the ε_{Ca} values ranged from +61.3 (biotite) to +1.6 (plagioclase).

8.12. PLEOCHROIC HALOES

These are zones of discoloration surrounding uranium- and thorium-bearing inclusions in minerals caused by the interaction of alpha-particles with atoms in the relevant crystal lattices resulting in their displacement or the displacement of constituent electrons from equilibrium positions. They comprise concentric rings with radii usually *ca* 10 to 50 μm. These radii record the kinetic energies of the alpha-particles involved and form because their ionizing power maximizes near the end of their ranges in particular media. (See Figure 4.1 in Chapter I.) Biotite is an optimal mineral in which to examine them since it has perfect cleavage and also such radiation damage discoloration is easily seen in it. Very energetic particles create giant haloes up to 110 μm across and are emitted, e.g. by ^{212}Po (10.5 MeV energy), a daughter of ^{232}Th. Larger haloes may perhaps be the result of the radioactive decay of super-heavy elements with atomic numbers up to 127. Pleochroic haloes have been used to date minerals and rocks. The approach depends on the fact that the intensity of their colours increases with the alpha dose to which they have been exposed and there are 3 stages involved. In the first, colour increases linearly with radiation dosage. A second is that of saturation in which the colour reaches a maximum density and does not increase further with increasing radiation dosage. The third is an inversion phase in which coloration decreases with intensity of radiation dosage and arises from extreme radiation damage. Only the

first stage minerals can be used in age determinations. It involves the assumptions that coloration really is a linear function of alpha dosage and that the concentrations of radionuclides emitting the particles have not altered except through radioactive decay. Practically, it is necessary to measure the alpha activity of the inclusion at the center of a pleochroic halo and assess its color intensity. Also, the relationship between these two parameters must be established and this may be done by irradiating the rnineral with particles from an artificial source or by examining similar haloes in other samples ot the mineral which are of known age. A drawback to the method is that haloes may be erased to some extent by metamorphism [31,32].

8.13. RADIOCARBON

Radiocarbon is produced in the atmosphere through the impact of cosmic ray neutrons on a small proportion of ^{14}N atoms thus: $^{14}N(n,p)^{14}C$, the ^{14}C then becoming incorporated into molecules of CO_2 by reaction with O_2 or by exchange with stable C isotopes in molecules of CO or CO_2. Molecules of $^{14}CO_2$ rapidly mix into atmosphere and hydrosphere to attain a constant level of concentration representing a steady state equilibrium maintained because of the continuous production of ^{14}C and its on-going radioactive decay thus:$^{14}C \rightarrow {}^{14}N+\beta^{-}+\bar{\nu}Q$, where Q=0.156 MeV and the ground state of ^{14}N is reached directly without γ-emission. There have been systematic variations in the radiocarbon content of the atmosphere in the past which cause inaccuracies where dating is concerned. One reason for such variations is that the rate of formation by the (n,p) reaction depends mainly on the density of the cosmic ray produced neutron flux which increases with altitude to attain a maximum between 12,000 and 15,000 m above the Earth's surface. Also the flux is greater by a factor of 4 in polar regions than at the equator. Consequently, the rate of production of ^{14}C is significantly higher at the poles which should mean that living tissues there ought to have more radiocarbon in them than those at the equator. However, some research has shown that specific ^{14}C activity may be independent of location perhaps because rapid mixing in the upper atmosphere, a process thought to last less than 2 years, reduces the effect to produce unifomity at the surface of the Earth. Also, the neutron flux will vary as the intensity of the solar proton flux does so that the ^{14}C content of the atmosphere doubtless varied with time as a function of alternating solar activity. In addition, the cosmic ray flux is modified by changes in the terrestrial magnetic field during the past 40,000 a or so. But data have been published which imply that the initial radiocarbon in a set of archaeologically dated samples was compatible with present values [33]. The radioativity of a C sample from a plant or animal tissue which died t years ago is given by $A=A_0e^{-\lambda t}$, where A is the specific activity at the present moment and A_0 is the specific activity of ^{14}C in the same sample when death occurred. A value for the estimated specific activity of ^{14}C was 226±1.2 Bq/Kg and the half-life, $T_{1/2}$, was given as 5730±40 a with a decay constant of 1.209×10^{-4} [34,35]. A "dead" sample containing C which is no longer in equilibrium with the ^{14}C of the atmosphere by solving the above equation for t thus:

$$\ln\left(\frac{A}{A_0}\right) = -\lambda t$$

$$t = \frac{1}{\lambda}\ln\left(\frac{A_0}{A}\right) \tag{8.13.1}$$

and substituting the value of λ gives:

$$t = 19.035\times10^{3}\ln\left(\frac{A_0}{A}\right)\text{a}$$

the accompanying Figure 8.13.1 showing the relationship between the ^{14}C activity of a sample and the time which has elapsed since exchange ceased with the reservoir. Several assumptions are made. The initial activity is taken to be a known constant independent of passing time through the past 70,000 a with a value independent of geographical location and the species of dead plant or animal from which the relevant tissue samples are taken. Also it is assumed that the sample to be

dated has not been contaminated by modern ^{14}C and that its observed activity is unaffected by radioactive impurities. Research has demonstrated that the initial ^{14}C activity of modern plant and animal tissues is constant to a first approximation and that the activity of radiocarbon in archaeological materials of known age is measurable with sufficient precision to provide ^{14}C dates agreeing satisfactorily with these historical ages.

Materials suitable for radiocarbon dating include charcoal, wood, grains, seeds, grasses, paper, hide, burnt bonea, cloth, peat, ivory, collagen, inorganic C in shells, organic C in shells, lake marl, lake and deep sea sediments, pottery and iron. Quantities required for analysis vary from *ca* 25 g for wood to 5,000 g for iron. To measure the ^{14}C contents, liquid scintillation has been used and is adequate for dates <30,000 a old. Ultra sensitive high voltage tandem mass spectrometers offer direct counting of ^{14}C ions but this technique is expensive.

It has been shown that the radiocarbon content of the atmosphere varied systematically in the past so that the ^{14}C activity *ca* 1700 and 1500 was *ca* 2% more than in the 19th century. This phenomenon is termed the **de Vries effect** [36]. Another such effect is manifested by a *ca* 2% drop in the activity of 20th century wood due to the introduction of "dead" CO_2 into the atmosphere

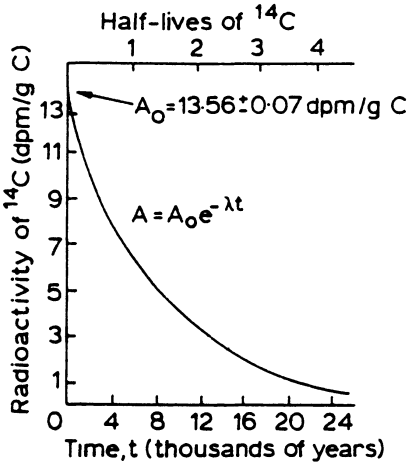

Figure 8.13.1. This illustrates the radioactive decay of radiocarbon in plant or animal tissues originally in equilibrium with atmospheric or hydrospheric $^{14}CO_2$ molecules; exchange ceases after the deaths of the organisms involved. The radioactivity diminishes as a function of time ($T_{1/2}$ for ^{14}C=5730±40 a). Iœ the residual radio-carbon activity is measured, the age, *t*, of the specimen is obtainable from this graph.

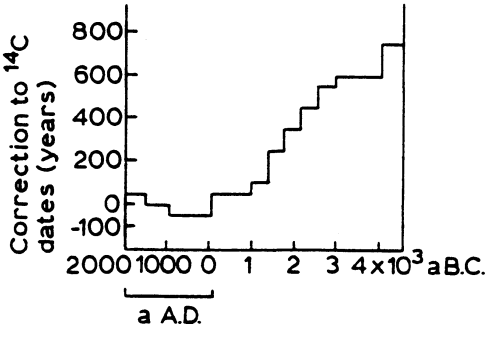

Figure 8.13.2. The graph gives corrections which have to be added to radiocarbon dates in order to bring them into agreement with tree ring dates based on 143 analyses of the wood of bristlecone and sequoia which yielded dendrochronological dates. The systematic deviations in the radiocarbon dates resulted from variations in the content of ^{14}C in the atmosphere through the past 6 ka.

through the combustion of fossil fuels after the start of the Industrial Revolution [37]. This so-called **Suess effect** was exceeded by the detonation of thermonuclear devices in the atmosphere and by the operation of nuclear reactors and particle accelerators. Bomb-produced radiocarbon is detectable in the oceans and also in the biosphere.

Analyzing old trees facilitated investigation of the secular variation of the ^{14}C content of the atmosphere. Such trees can be dated using tree rings, annual accretions of woody tissue to the circumferences of their trunks. And layers deposited earlier cannot absorb ^{14}C from the atmosphera any more so that their radiocarbon contens decrease by radioactive decay. Two tree genera were used, namely *Pinus aristato* and *Sequoia gigantea* (the bristlecone pine and the sequoie.). Combining dendrochronology with isotopy enabled age-corrected deviations of the ^{14}C contents of such trees to be utilized in calculating corrections applicable to conventional radiocarbon dates, v. accompanying Figure 8.13.2. The problem with the approach is that dendrochronology only goes back *ca* 12,000 a into the past. However, examination of the varve chronologies of sediments deposited in glacial lakes extends radiocarbon dating further back. Research seems to indicate that the ^{14}C content of the atmosphere varied by *ca* ±10% of the 19th century value. Radiocarbon is important for dating groundwaters, an application first proposed in 1957 [38]. This was done on the basis that soil zone CO_2 is biogenic in origin, resulting from the respiration of plant roots and also from the decay of plants. Hence it contains radiocarbon from the atmosphere. The actual content of the radioisotope decays steadily since the gas is no longer in contact with the atmosphere and the fraction of the original content still remaining is a measure of the time elapsed since this happened through infiltration. The time since this took place, t, is given by:

$$t = 8270 \ln(C_0 / C) \text{a} \qquad (8.13.2)$$

where 8270 a is the mean life of radiocarbon C_0 is the initial concentration of the ^{14}C and C is the concentration recorded in the sample. Because radiocarbon is measured relative to the total C content of the sample, the origin of the stable C present must be examined as well. Not all of it is similar in origin to the ^{14}C (i.e. atmospheric) since infiltrating water contains CO_2 dissolved out of the soil zone which dissolves carbonate minerals in the soil:

$$H_2CO_3 \rightleftarrows HCO_3^- + H^+$$

$$CaCO_3 + H^+ \rightleftarrows HCO_3^- + Ca^{2+}$$

However, water from limestones contains no radiocarbon, hence that reaching the water table contains dissolved C in the chemical forms H_2CO_3, HCO_3^- and CO_3^{2-} with a radiocarbon content lower than that occurring in the soil (biogenic) CO_2. The evaluation of the dilution of soil CO_2 originally containing 100% modern ^{14}C with ^{14}C-free ("dead") carbonate in order to estimate the initial radiocarbon concentration in recharge water reaching the water table is one of the most difficult problems of ^{14}C age determination.

Fractionation of the C isotopes in nature entails small systematic errors in radiocarbon dates which can be eliminated when the isotopic composition of stable C to be dated can be assessed using a mass spectrometer. This value is expressed as $\delta^{13}C$. Such fractionation during photosynthesis alters the abundances of the stable isotopes ^{12}C and ^{13}C from those prevailing in the atmosphere and plants usually become enriched in ^{12}C and depleted both in ^{13}C and ^{14}C.

Thermonuclear bomb-produced radiocarbon has been used to trace ocean and aquifer circulation patterns and also to calculate air/sea exchange. Until recently, the variation of bomb ^{14}C in oceans was restricted to analysis of banded corals and so to lower latitudes. A shell-derived chronological history of bomb ^{14}C on Georges Bank and its Labrador Sea implications offered high latitude data resulting from analysis of a 54 a old mollusc (age determined from annual growth bands) using accelerator mass spectrometry [39]. This gave a time history from 1939 to 1990. This widened the scope of investigation. Other significant information came from the southern Great Barrier Reef in Australia [40]. Radiocarbon and stable isotope ($\delta^{18}O$ and $\delta^{13}C$) data for biannual samples were obtained from a 323 a banded coral series collected from this region. The high precision $\Delta^{14}C$ record showed variations on an inter-annual time scale which were especially large from 1680 to 1730. This may have nothing to do with atmospheric changes, but rather to have involved changes in vertical mixing and large scale advective changes of source waters to the western Coral Sea. Low values from 1635 to 1875 may relate to El Niño/Southern

Oscillation events in the eastern tropical Pacific. But these cannot explain all the variations, especially those from 1875 to 1920 characterized by high $\Delta^{14}C$ values. The time interval 1635 to 1795 appears to embody a 6-a periodicity, a coherency later lost. It may be inferred that secular changes take place in the nature and properties of the El Niño/Southern Oscillation as manifested in the southwestern Pacific. Interestingly, no trace of the **Suess effect** was found from the coral record.

8.14. RHENIUM/OSMIUM

The beta decay scheme of ^{187}Re to ^{187}Os is applicable to studying sulphide minerals of molybdenum and Os-rich minerals such as iridosmine. With Rb/Sr, Sm/Nd, Lu/Hf and U/Pb methods, it has been utilized to examine mantle differentiation and the accretion of continental crust. In molybdenites, Re concentrations vary from a few ppm to as much as 1.88% The element has 2 naturally occurring isotopes, the stable ^{185}Re with a relative abundance of 37.398% and radioactive ^{187}Re with a relative abundance of 62.602±0.016%. This decays as follows: $^{187}Re \rightarrow {}^{187}Os + \beta^- + y + Q$, Q being *ca* 2.5 keV. This makes it difficult to determine its half life by direct counting, but it is *ca* 4.56 Ga and its decay constant *ca* $1.64\pm0.05\times10^{-11}$ a^{-1}. The growth of Os in a rhenium-bearing system may be expressed thus:

$$\frac{^{187}Os}{^{186}Os} = \left[\frac{^{187}Os}{^{186}Os}\right]_i + \frac{^{187}Re}{^{186}Os}\left(e^{-\lambda t} - 1\right)$$

where the first term is the ratio of the isotopes now, the second is that which prevailed originally (when the system closed to both elements) and the third includes the present ratio of ^{187}Re to ^{186}Os; λ is the decay constant. Of course, the second term must necessarily be an assumption. The equation can be applied to a suite of samples with a common age and presumably the same initial [$^{187}Os/^{186}Os$] ratio and these form an isochron in coordinates of $^{187}Os/^{186}Os$ and $^{187}Re/^{186}Os$ of which the relevant slope is proportional to their age. The zero intercept of the isochron will give the initial [$^{187}Os/^{186}Os$] ratio. Concentrations of both elements have been determined in iron meteorites and these plus the metallic grains of chondrules were found to fit the same isochron which implies that they formed within a very short time interval, estimated to be *ca* 90 Ma, from the solar nebula (thought to have contained isotopically homogeneous Os). The primordial $^{187}Os/^{186}Os$ ratio has been given as 0.807±0.006. And the isotopic compositions of both Re and Os in meteorites are compatible with terrestrial sample values.

The Re contents of molybdenites ranged from 2 to 230 ppm in 19 samples.

However, the Os content was <0.2 ppm, probably due to the presence of radiogenic ^{187}Os formed through in situ decay of ^{187}Re. Since it has a very high Re/Os ratio, molybdenite is particularly suitable for Re/Os dating and, for the above samples, ages ranging from 105 Ma, to 2.54 Ga were obtained. Osmium-bearing minerals may record the isotopic evolution of the element in the mantle as is implied by the genetic association of iridosmine with ultramafic rocks. Data have been published on measurements of $^{187}Os/^{186}Os$ ratios from iridosmine samples with known ages and, when shown in coordinates of $^{187}Os/^{186}Os$ and time, fitted a straight line with slope of 1.04±0.050768 t, where t = time. The collinearity of these data points indicates that the mantle sources of these samples must have had a homogeneous Re/Os ratio which altered solely due to the decay of ^{187}Re. The value of this ratio was calculated from the slope of the osmium-development line by taking $(e^{-\lambda t}-1)$ in the preceding equation as roughly λt. In this case, $^{187}Re/^{186}Os$ = slope/λ. And, if $\lambda=1.52\times10^{-11}$ a^{-1}, then the ratio in the mantle is 3.34±0.14 and the corresponding Re/Os ratio is *ca* 0.085. The intercept of the osmium-development line gives a value for the $^{187}Os/^{186}Os$ ratio in the mantle at present, i.e. at t=0, of 1.040±0.01. Both ratios in the mantle comprise the coordinates of a point lying on the Re/Os isochron for meteorites and the agreement suggests that the Earth and the parental bodies of the meteorites formed at about the same time from a primordial source containg Re and Os, both with a homogeneous isotopic composition.

Since a unique osmium-development line exists, it can be inferred that, despite internal magmatic activity accompanying formation of the crust, the mantle is homogeneous as regards its Re/Os ratio [41]. Granites, ultrabasics and basalts have similar Re concentrations, therefore the

element was not much partitioned during partial melting and fractional crystallization and the geochemical differentiation of the mantle could not have changed its Re concentration much. As Os is depleted in granites and basalts compared with ultramafics, it could be that only a small fraction of mantle Os has been transferred into the crust. And so, while the Re/Os ratio appears to have been fairly stable through time, the crust seems to have undergone more variation in it. Hence variability of it could be a useful indicator of crustal contamination of magma.

8.15. RUBIDIUM/STRONTIUM

Rb has an ionic radius sufficiently close to that of K that it can substitute for the latter in all potassium-bearing minerals and therefore occurs as a dispersed element forming measurable parts of micas, potassium feldspar, some clay minerals and evaporites. Two isotopes occur naturally, i.e. ^{85}Rb and ^{87}Rb with isotopic abundances of 72.17% and 27.83%, respectively, ^{87}Rb being radioactive, decaying to ^{87}Sr by negatron emission with $T_{1/2}$ =4.8×10^{10} a. This process may be described as follows:

$$^{87}Rb \rightarrow ^{87}Sr + \beta^- + \bar{\nu} + Q$$

where Q=0.275 MeV. Sr has 4 naturally occurring isotopes, ^{87}Sr having a relative abundance of 7% and a metastable state with a γ-energy of 388 keV for the isomeric transition. This decays by EC in a time interval determined by the half-life which is 2.81 h. The abundance varies, reflecting the formation of radiogenic ^{87}Sr by the decay of ^{87}Rb. Hence, the precise isotopic composition of Sr in a mineral or rock containing Rb depends on the age and the Rb/Sr ratio of either.

The growth of radiogenic ^{87}Sr in a rubidium-enriched mineral over a time interval t is given by:

$$^{87}Sr = ^{87}Sr_0 + ^{87}Rb(e^{-\lambda t}-1)$$

where ^{87}Sr and ^{87}Rb are the total numbers of atome of the respective isotopes in a unit mass of the mineral now and $^{87}Sr_0$ is the amount of ^{87}Sr incorporated in it when it crystallized, λ is the decay constant of ^{87}Rb and t represents the age of the mineral sample. Dividing each term by the number of ^{86}Sr atoms found (a constant, because this is a stable isotope) gives:

$$\frac{^{87}Sr}{^{86}Sr} = \left[\frac{^{87}Sr}{^{86}Sr}\right]_o + \frac{^{87}Rb}{^{86}Sr}\left(e^{-\lambda t} - 1\right)$$

which is the equation for age determination, assuming that the system remained closed after crystallization. Slightly variable values for the half-life of ^{87}Rb have been given, hence for the decay constant too, but 1.49×10^{-11} a^{-1} must be close to the true figure. Measuring Rb and Sr concentrations in suitable minerals may be done using standard chemical and mass spectrometric procedures, X-ray fluorescence or isotope dilution. In the mass spectrometer, the $^{87}Sr/^{86}Sr$ ratio is obtained utilizing a pure Sr salt derived by dissolving the mineral involved in acid and separating Sr through cation exchange chromatography. Ratios of the Rb and Sr concentrations are converted into $^{87}Rb/^{86}Sr$ ratios as follows:

$$\frac{^{87}Rb}{^{86}Sr} = \left(\frac{Rb}{Sr}\right)_c \frac{Ab\left[^{87}Rb\right]W_{Sr}}{Ab\left[^{86}Sr\right]W_{Rb}}$$

where Ab = abundance; the derived ratio is that between the nuclides involved given in terms of the numbers of atoms present in a unit mass of the mineral sample now:$(Rb/Sr)_c$ is the ratio of the concentrations of the elements and W = relative atomic masses. Since the abundance of ^{86}Sr and the relative atomic mass of the element depend on the abundance of ^{87}Sr, suitable values have to be determined for each individual mineral sample.

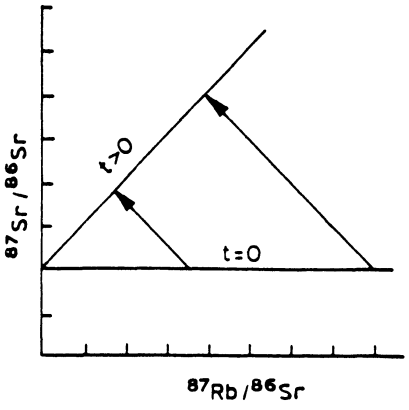

Figure 8.15.1. A rubidium/strontium diagram exhibiting the time-dependent isotopic evolution of rock systems after they crystallized from a homogeneous magma.

To solve the age equation for t, a suitable value for the $^{87}Sr/^{86}Sr$ ratio of that Sr which became incorporated into the mineral being analyzed when it formed must be used. An appropriate value has been given as 0.706, this being representative of a large number of recent basic volcanics. And any particular suite of co-magmatic rocks with an age t defines an isochron if its members all had the same initial $[^{87}Sr/^{86}Sr]$ ratio and were closed to Rb and Sr since crystallization. Optimally the whole rock isochron approach should involve a suite of which the members cover as broad a range of Rb/Sr ratios as possible so as to get a well defined slope for the relevant isochron. A straight line fit by regression analysis may be undertaken and both the slope and the intercept of the isochron determined. Whole rock Rb/Sr isochron data may be regarded as quite reliable age indicators, *v.* accompanying Figure 8.15.1.

8.15.1. Real and fictitious isochrons

Real isochrons may be altered through metamorphism when heating causes minerals to deviate from the whole rock isochron so that each acquires its own isochron. Also, new minerals may form and existing minerals may re-crystallize. The entire situation is of one mobility entailing ionic diffusion. Metasomatism may take place and involve both the bulk chemical composition and the trace element composition. This phenomenon can affect parent-daughter relationships of all naturally occurring radioactive element systems in a particular rock. Bearing these considerations in mind, the following expression may be given:

$$t = \frac{2.303}{\lambda} \log \left[\frac{\frac{^{87}Sr}{^{86}Sr} - \left[\frac{^{87}Sr}{^{86}Sr}\right]_o}{\frac{^{87}Rb}{^{86}Sr}} + 1 \right] \qquad (8.15.1)$$

from which t may be obtained. The best rocks to use appear to be igneous acidic ones such as granite because they contain both micas and potassium feldspars. However, both concordant and discordant results may be obtained. The latter are due to gain or loss of radiogenic ^{87}Sr caused by geological events usually associated with metamorphism. And when forming, such igneous rocks undergo fractional crystallization of magma entailing the separating of crystals from an ever-diminishing liquid magma, hence suites of co-magmatic igneous rocks have different chemical compositions. But if it be assumed that the Sr in such a magma stayed isotopically homogeneous through cooling, all the various suites formed will have the same initial $[^{87}Sr/^{86}Sr]_o$ ratio. It is acceptable to assume that all rocks formed will have roughly the same age because cooling and

crystallization times are negligible compared with the age of the event. In this way, the age equation may be looked on as pertaining to a set of suites and creating a group of straight lines on a plot having a slope intercept form such that $y=b+mx$. All rock samples from a co-magmatic suite plot as points on a straight line in coordinates of $^{87}Sr/^{86}Sr$ (y) and $^{87}Rb/^{86}Sr$ (x), i.e. form an isochron. Its slope is related to t thus:

$$m = e^{-\lambda t} - 1$$

and the value of the initial $^{87}Sr/^{86}Sr$ ratio is provided by the y intercept. Fictitious isochrons have slopes devoid of geochronological significance. If a set of samples resulted from the mixing of two components with different $^{87}Rb/^{86}Sr$ and $^{87}Sr/^{86}Sr$ ratios, they will fall on a straight line which links the end members in coordinates of these ratios. Such a straight line is a fictitious isochron and it may have a positive or negative slope depending on the relative values of the end members. An instance was obtained from potassic lava flows found in volcanic centres lying along the western Great Rift Valley north of Lake Tanzania and west of Lake Victoria, these centres being *ca* 160 km apart [42]. Identified as Pliocene to Recent in age, their volcanic activity is believed to have continued into historic times so there is no doubt that the relevant rocks are young and ought to give an isochron with practically zero slope. However, a significant positive correlation between the average $^{87}Sr/^{86}Sr$ and the $^{87}Rb/^{86}Sr$ ratios of the various rock types was found and the straight line drawn through the data points was no isochron, rather a mixing line. It had a slope yielding a fictitious age of 773 Ma because the $^{87}Sr/^{86}Sr$ ratios of the rocks resulted from mixing and do not relate to the radioactive decay of ^{87}Rb in them after crystallization.

Rb/Sr analyses of chondritic meteorites have given an average age of *ca* 4.49 Ga as did those of achondrites and it has been suggested that crystallization took place rapidly and that they had similar initial [$^{87}Sr/^{86}Sr$] ratios. Basaltic achondrites gave a value for the primordial $^{87}Sr/^{86}Sr$ ratio of 0.69897±0.00003 and this is termed BABI (basaltic achondrite best initial). Isotope anomalies in meteorites imply that the solar nebula could not have been isotopically homogeneous with respect to some elements. The concert of *F*ractionation and *UN*known effects as possible causes produced the term FUN [43]. The Rb/Sr method has been used to help unveil the selenological history of the Moon and an age for the satellite of *ca* 4.5 Ga was obtained. BABI is paralled by LUNI of which the value has been given as 0.69892±0.00009 [44].

8.16. SAMARIUM/NEODYMIUM

Both Sm and Nd are lanthanides (rare earth elements) and each has 26 isotopes of which 7 occur naturally. ^{147}Sm is radioactive and decays by α-emission to a stable isotope of Nd, ^{143}Nd. Its half-life is 1.06×10^{11} a with a corresponding decay constant of 6.54×10^{-12} a^{-1} and the decay scheme is applicable to dating terrestrial rocks, stony meteorites and lunar materials. These and the other rare earth elements occur in high concentrations in minerals such as monazite ($CePO_4$) and as trace elements in common rock-forming ones such as biotite and plagioclase feldspar. Relative abundances of these elements in the solar system have been given as 2.61×10^{-1} atoms per 10^6 Si atoms for Sm and 8.36×10^{-1} atoms per 10^6 Si atoms for Nd, the lower abundance of Sm according with the general decrease of the cosmic abundances of the elements with increasing atomic number. The atomic Sm/Nd ratio in the solar system is 0.31 and on Earth varies from 0.1 to 0.5. The relative abundances are 15% for ^{147}Sm and 12.18% for ^{143}Nd. It has been inferred that Nd is concentrated more than Sm during the fractional crystallization of magma and that crustal rocks usually have lower Sm/Nd ratios than rocks originating from the upper mantle such as oceanic tholeiites. Also, during the formation of silicate liquids by partial melting of rocks in the crust or mantle of the Earth, the liquid phase may enrich in Nd relative to Sm. Possibly this is because Nd^{3+} has a larger ionic radius than Sm which gives it a lower ionic potential as a result of which it forms weaker ionic bonds that can be more easily ruptured than those of Sm^{3+}. The geochemical characteristics of the two elements can be described in terms of their distribution coefficients D_l^m thus:

$$D_l^m = \frac{C_m}{C_l}$$

pressure, oxygen fugacity and chemical composition of the liquid. Therefore, there is occasional disagreement between empirical partition coefficients and those obtained by analyzing phenocrysts and the matrices of porphyritic volcanics. It has been shown that such partition coefficients of the rare earth elements for clinopyroxene satisfy the following expression:

$$\log_{10} D_i^m = a \log_{10} \frac{\text{Fe}}{(\text{Fe} - \text{Mg})} + b$$

where Fe/(Fe–Mg) is the atomic ratio in the clinopyroxene and a and b are constants (1.438 and 0.670 for Sm and 1.348 and 0.438 for Nd). Therefore, the partition coefficients of a clinopyroxene in which Fe/(Fe–Mg)=0.2 are D(Sm)=0.46 and D(Nd)=0.31.

Sm and Nd are interrelated by parent-daughter links through the α-decay process by which ^{143}Nd derives from ^{147}Sm and by the decay from ^{146}Sm which results from the α-decay of ^{150}Gd to the stable nuclide ^{142}Nd. Thus:

$$^{147}\text{Sm} \rightarrow ^{143}\text{Nd} + \alpha + Q\left(T_{1/2} = 1.06 \times 10^{10}\text{a}\right)$$

$$^{150}\text{Gd} \rightarrow ^{146}\text{Sm} + \alpha + Q\left(T_{1/2} = 1.80 \times 10^{6}\text{a}\right)$$

$$^{146}\text{Sm} \rightarrow ^{142}\text{Nd} + \alpha + Q\left(T_{1/2} = 1.00 \times 10^{8}\text{a}\right)$$

Q being the decay energy.

The radioactive decay of ^{147}Sm and the growth of radiogenic ^{143}Nd may be expressed as follows:

$$\frac{^{143}\text{Nd}}{^{144}\text{Nd}} = \left[\frac{^{143}\text{Nd}}{^{144}\text{Nd}}\right]_o - \frac{^{147}\text{Nd}}{^{144}\text{Nd}}\left(e^{-\lambda t} - 1\right)$$

where ^{144}Nd acts as the reference since the number of its atoms in a unit quantity of any given sample remains constant so long as the host system remains closed to Nd. The decay constant, λ, is taken as 6.54×10^{-12} a^{-1}. Determination of ages by the Sm/Nd method entails analyzing either individual minerals or co-genetic rock suites in which the ratios between the two are sufficiently diverse to define the slope of an isochron in coordinates of ^{143}Nd/^{144}Nd and ^{146}Sm/^{144}Nd. The method is especially suitable for mafic and ultramafic rocks, cf. the Rb/Sr method which is best suited for acidic and intermediate igneous rocks enriched in Rb and depleted in Sr. Since the rare earth elements are less mobile than the alkali metals and the alkaline earths, phenomena such as regional metamorphism have less effect on them. Hence suitable rocks can be dated by the Sm/Nd method even if they have lost or gained Rb and Sr. This makes the Sm/Nd method a useful complement to the Rb/Sr method.

Volcanics from the Onverwacht Group, Swaziland and South Africa, comprise the basal part of the Early Precambrian Barberton greenstone belt found in Swaziland and the Transvaal. Data, from them gave an age of *ca* 3.54 Ga which was calculated using an initial $[^{143}\text{Nd}/^{144}\text{Nd}]_o$ ratio of 0.50809±0.00004 [45]. The Sr and Nd isotopic record of *Apollo 12* basalts from the Moon has been examined as well. Isochrons have been presented for an achondrite (eucrite) and another meteorite and gave ages of *ca* 4.58 Ga and 4.562 Ga with primordial ^{143}Nd/^{144}Nd ratios of 0.50684±0.00008 and 0.506664. An initial $[^{87}\text{Sr}/^{86}\text{Sr}]_o$ ratio was termed ADOR. The isotopic evolution of Nd in the Earth has been described by means of a model termed CHUR (*CH*ondritic *U*niform *R*eservoir) and the present value of the ^{143}Nd/^{144}Nd ratio is 0.512638 relative to a ^{146}Nd/^{144}Nd ratio of 0.7219. The present value of the ^{147}Sm/^{144}Nd ratio of CHUR is 0.1967 which allows calculation of the ^{143}Nd/^{144}Nd ratio of CHUR in any past time interval from the following equation:

$$I^{pa}\text{CHUR} = I^{pr}\text{CHUR} - \left[\frac{^{147}\text{Sm}}{^{144}\text{Nd}}\right]^{pr}_{\text{CHUR}} \left(e^{\lambda t} - 1\right)$$

where I^{pa}CHUR is the $^{143}Nd/^{144}Nd$ ratio of CHUR at a past time t, I^{pr}CHUR is the present ratio, i.e. 0.512638 normalized to $^{146}Nd/^{144}Nd$=0.7219, and $[^{147}Sm/^{144}Nd]^{pr}_{CHUR}$ is the present value based on analyses of meteorites (=0.1967). An ε parameter was introduced and can be either positive or negative. Where positive, it denotes that samples originated from residual solids in the reservoir after early magma withdrawal and where negative, it indicates that samples came from sources with a lower Sm/Nd ratio than the chondritic reservoir and either stemmed from or incorporated old crust of which this ratio had been lowered on separating from CHUR.

8.17. THERMOLUMINESCENCE (TL)

This phenomenon results from the increase in temperature of a body and occurs when electrons trapped in crystal defects are released by heat. When ionizing radiation impinges on a dielectric solid, electrons may be stripped off and so become trapped in metastable states associated with the said defects. Heat frees this energy as light emission when the trapped electrons resume their stable ground states. Such light emissions are quite independent of the normal incandescence shown by thermally activated solids and increase linearly with the radiation dose until saturation is reached. Once electron traps are drained by heating, TL disappears unless the sample is irradiated again. In TL dating, a sample is heated at increasing temperatures and its light output recorded as a glow curve, the area under which measuring the radiation dose to which the sample was subjected since it was last heated to *ca* 450 °C. The annual radiation dosage can be determined from the concentrations of U, Th and K in the rock sample and the time elapsed since the last heating, t, is given by:

$$t = \frac{\text{accumulated radiation dose}}{\text{annual radiation dose}} \tag{8.17.1}$$

The accumulated radiation dose is given by the glow curve. In the 1950s, it was suggested that the method could be used to date geological materials and shown that TL can be induced by pressure and the recrystallization of solids. Later archaeological materials and even Pleistocene sediments have been analyzed and gave important information. TL dates have been obtained from loess deposits above and below the Old Crow tephra at the Halfway House site near Fairbanks, Alaska, and its age restricted to 86±8 ka which accorded with radiocarbon records from wood and peat less than 6 m above the tephra yielding an age of over 60 ka [46]. Emission spectra of meteorites showed that neither trapping levels at 170 °C and 350 °C nor the luminescence centers were significantly perturbed by either their shock or thermal histories. A tentative assignment of the luminescence producing the lower temperature broad emission feature was made to Mn^{2+} ions in the oligoclase feldspar [47].

8.18. TRITIUM

Tritium, ^{3}H, is produced in the atmosphere by the interaction of cosmic ray-produced neutrons with a small portion of the N thus:

$$^{14}N + n \rightarrow {}^{3}H + {}^{12}C$$

and also results from solar emissions, operation of nuclear reactors and particle accelerators on Earth and a diminishing residue caused by earlier atmospheric detonations of thermonuclear devices. Tritium has a half life of 12.3 a and decays with β^--emission to ^{3}He. The rate of natural production is *ca* 0.25 atom cm^{-2} s^{-1} [48]. Once formed, the radioisotope is rapidly incorporated into water molecules and resides in the lower stratosphere for anything between one and ten a. Later, such molecules enter the lower troposphere and rainout of the tritiated water (HTO) occurs within five and twenty d. This is how HTO enters the hydrologic cycle where it constitutes a radio-tracer for water which has been in the atmosphere for the past 35 a. However, as the bomb

component decreases, so does the radiotracing value. The ^{3}H content of natural waters is given in tritium units, TU, of which one is equal to an abundance of 1 atom of tritium per 10^{18} atoms of ^{1}H (= 118 Bq of ^{3}H per m^3 of water). This extreme dilution means that measuring ^{3}H contents in water necessitates preliminary enrichment of the radioisotope. In practice, 1 TU is about the lowest quantity which can be detected. Cosmic ray-produced tritium established a pre-bomb level of *ca* 10 TU in temperate zone meteoric waters (assessed using wine samples of suitable age because these depend not just on water intake, but also on the atmospheric water content exchanging with the grapes). Indeed, wine samples laid down before the thermonuclear bomb era represent the only undisturbed and well dated samples of atmospheric water from those times since part of the water content came from tropospheric moisture. After 1953, the tritium content in precipitation increased through bomb testing to reach values as high as 10,000 TU in the northern hemisphere by 1963. Thereafter, they fell off to a more or less stable value persisting until today and just above the pre-1953 level.

Tritium in precipitation is used to establish the input into groundwater systems, although seasonal changes and evapotranspiration in vegetated areas affect this by returning most of the radioisotope to the atmosphere. Where no tritium is present in groundwater, it is clear that recent recharge water has not reached the sampling point. On the other hand, if tritium is present, water less than 20 a old has penetrated to it. Usually a mixture of waters from several sources is involved and may include young water containing tritium and old, tritium-dead, water. Another possibility is that of a water sample having a tritium content which is constant with time. This would show good mixing between young and old waters with the size of an aquifer masking the fluctuation due to recharge. So in groundwater studies, tritium measurements produce data on the time of recharge to an aquifer system [49]. A well mixed reservoir shows exponential discharge and a mean residence time for water in it can be estimated [50].

Tritium has been used too in order to study the downward progress of water in the unsaturated zone en route to recharging a groundwater system. Tritiated water, enriched in ^{2}H as well as ^{3}H, labelled a specific horizon of soil moisture and its rate of downward movement and the dispersion of the radiotracer were monitored in core samples taken from the test plot [51].

It may be added that the observed content of ^{3}H in meteorites has been used to estimate their ages (termed $^{3}H/^{3}He$ age) and the method was to divide the observed total number of ^{3}He atoms by the number of ^{3}H atoms decaying per unit time and making a correction of *ca* 30% for the directly produced ^{3}He. Results were not certain, partly because of the necessity of assuming that there was a constant ^{3}H content, or constancy of the cosmic ray flux at the meteoroid integrated over 25 a.

8.19. URANIUM SERIES DISEQUILIBRIUM DATING

8.19.1. Ionium

Ionium, ^{230}Th, is a daughter of ^{234}U and produces ^{226}Ra in the ^{238}U radioactive decay series. Its half-life is 7.52×10^{4} a and the corresponding decay constant is 9.217×10^{-6} a^{-1}. Differences in geochemical properties induce Th isotopes to separate from U in the oceans which is the basis of using ionium to date deep sea sediments. In oxidizing conditions on the Earth's surface, U occurs as the uranyl ion, UO_2^{2-}, whereas Th remains tetravalent and is rapidly abstracted from sea water by adsorption on solid surfaces and also by incorporation into authigenic minerals (U concentrating in the aqueous phase). Hence the residence time of U in oceans is longer by orders of magnitude than that of Th – *ca* 0.5 Ma compared with *ca* 300 a. Most ionium in sea water is the result of decay, but *ca* 25% is believed to come from river input. The preferential removal of ionium from sea water separates the radio-nuclide from its parent and produces an excess of unsupported ionium in the sediments. This causes activity which falls off with time, this assuming that both decay-formed and river-derived components are removed altogether from sea water. A sample of sediment from a given depth below the water-sediment interface can be dated from its $^{230}Th/^{232}Th$ ratio if this has stayed constant for at least several hundred thousand a in the water body next to the sediment in any given ocean basin and also if there was no migration of the isotopes in the sediment. In addition, their chemical speciation must have been the same in sea water with no isotopic fractionation between this and the mineral phases involving Th in the sediment. Furthermore, the ionium and Th found in detrital mineral particles must be excluded from the

analysis. Assuming that the contribution made by uranium-supported ionium is negligible, the activity of a sample, given as an activity ratio R, may be related to its age thus:

$$R = R_0 e^{-\lambda t}$$

where R is the ionium/thorium activity ratio of the leachable fraction of sediment obtained at a given depth below the top of a core, R_0 is the same ratio for newly deposited sediment, λ is the decay constant of ionium and t is the time elapsed since deposition occurred. R is measured and, if R_0 is known, then:

$$t = \frac{1}{\lambda} \ln \frac{R_0}{R} \qquad (8.19.1)$$

The approach has been used to determine the rate of sedimentation in open oceans. This varies greatly due to such factors as the amount of detritus introduced by rivers, the rates of melting of icebergs and the numbers of particles transported through and deposited by the atmosphere. The ionium/thorium method covers a range from less than 0.5 mm per 10^3 a to 50 mm per 10^3 a on a carbonate and opal-free basis, the lower figures applying in the South Pacific and the higher in the Atlantic. This is paralleled by variation in $^{230}Th/^{232}Th$ activity ratios on the surfaces from which it has been inferred that there is a greater input of ^{232}Th in the Atlantic perhaps due to the many large scale rivers entering it. But an excess ^{230}Th method may be applicable for separating ocean sediments into fractions which form isochrons of which the intercepts decrease with depth in the core. However, the slope of the isochron in young samples was found not to be zero, as expected, but rather showed a disequilibrium among the Th isotopes in the sediment [52].

8.19.2. Ionium/Protactinium

Pa, is a radioactive element with 21 isotopes of which the one of interest is ^{231}Pa with a half life of 32,480 a and a corresponding decay constant of 2.134×10^{-5} a^{-1}. It is a daughter of ^{231}Th in the ^{235}U radioactive decay series. In oceans, its geochemical properties resemble those of Th since the isotopes are removed from sea water either by adsorption on mineral grains or by incorporation into authigenic minerals. Thus sediments deposited in oceans may contain not only excess unsupported ^{230}Th, but also unsupported ^{231}Pa. If both are removed equally efficiently from sea water, then their activity ratios will alter with time in a manner controlled by their decay constants:

$$\left[\frac{^{230}Th}{^{231}Pa}\right]_{Ax} = \left[\frac{^{230}Th}{^{231}Pa}\right]_{Ax}^{o} \frac{e(-\lambda_{230}\, t)}{e(-\lambda_{231}\, t)}$$

in which the left-hand side represents the activity rate of the unsupported ionium and ^{231}Pa per unit mass of sediment at a time t, the second ratio relates to the time of deposition and the decay constants are those of ionium and ^{231}Pa. In this expression, it is assumed that the U concentration in the leachable fraction can be neglected. If this is so, then the unsupported ionium/^{231}Pa activity ratio is given by:

$$\left[\frac{^{230}Th}{^{231}Pa}\right]_{Ax} = \left[\frac{^{230}Th}{^{231}Pa}\right]_{Ax}^{o} e^{-\lambda' t}$$

where $\lambda' = \lambda_{231} - \lambda_{230} = 12.123\times10^{-6}$ a^{-1}. Clearly, therefore, the ratio of the activities of the unsupported ionium and ^{231}Pa increases with depth in a core. If the sediment is deposited at a uniform rate, then:

$$\ln\left[\frac{^{230}Th}{^{231}Pa}\right]_{Ax} = \ln\left[\frac{^{230}Th}{^{231}Pa}\right]_{Ax}^{o} + \frac{\lambda' h}{\alpha}$$

where h is the depth in the core and α is the constant rate of sedimentation (h/t). This is a straight line equation in coordinates of h and $\ln(^{230}Th/^{231}Pa)_{Ax}$. Its slope will be inversely proportional to

the rate of sedimentation and its intercept equals the initial value of the activity ratio of the relevant unsupported ionium and ^{231}Pa in the sediment. This approach has been used to determine α for a core from the Arctic Ocean and a value of 0.2 cm per 10^3 a was derived [53]. Later it was found possible to date one sediment sample only so that dating a whole suite of samples became unnecessary [54]. If is the time interval between the production of ^{231}Pa and its incorporation into a sediment, then:

$$^{231}Pa_A = {}^{235}U_A\left(1 - e^{-\lambda 231 t}\right)$$

and the growth of ionium from ^{234}U in sea water is similar.

8.19.3. Lead-210

In the uranium series, a daughter of ^{238}U is ^{222}Rn which enters the atmosphere at a rate of *ca* 42 atoms m^{-1} cm^{-2} of land surface and later decays through several short lived daughters to ^{210}Pb (half life 22.3 a). This is then removed by precipitation, having a residence time of only *ca* 10 d. Later the radionuclide is deposited in snow and ice in glaciers as well as in lakes and coastal regions. The activity of unsupported ^{210}Pb thereafter diminishes as a function of time at a rate determined by the half life. ^{210}Pb is useful for dating materials originating within the last 100 a which contain it and it has been used for measuring the rates of deposition of snow in Greenland and Antarctica as well as on Alpine glaciers. And lake sediments have been dated too, e.g. those of Loch Lomond in Scotland [53].

In addition to the unsupported (excess) ^{210}Pb of atmospheric origin, the radio-nuclide is found in unsupported form in sediment minerals, i.e. at equal activity to its parent by in situ production from the decay of ^{226}Ra. This component is controlled by sediment mineralogy and so yields no time scale information. The unsupported ^{210}Pb is quantified by subtracting the measured activity of supported ^{210}Pb from the total ^{210}Pb inventory at each depth in a core. ^{222}Rn activity is measured and the total inventory assessed by analysis of ^{210}Pb decay products ^{210}Bi or ^{210}Po. In all cases, secular equilibrium is assumed for the parent-daughter pairs. Thus the conventional dating method is indirect and specialized, involving nuclear counting equipment and radiochemical expertise. A more practical alternative is afforded by a particle track approach which is dependent on counting radiation damage tracks produced in selected plastic films by both alpha-particles and fission products emitted from essentially unprocessed dried sediment. Supported ^{210}Pb is measured indirectly by ^{235}U analysis. Because the $^{235}U/^{238}U$ ratio does not vary significantly in nature, the ^{238}U content of a sample can be calculated and secular equilibrium with ^{210}Pb again invoked. The supported ^{210}Pb profile is then subtracted from the total alpha record and the assumption made that the resultant excess alpha-plot is dominated by the decay of unsupported ^{210}Pb (or ^{210}Po). Using this method depends on an idealized non-migratory behavior for all other U series alpha-emitters and on total constancy with depth of ^{232}Th and its decay products.

As regards snow and ice chronology, the time elapsed since a sample of snow deposited at a depth h from the surface can be calculated from the activity of ^{210}Pb if the initial activity of this radionuclide has remained constant so that:

$$^{210}Pb_A = {}^{210}Pb_A^0\, e^{-\lambda t}$$

where the first term expresses the activity per unit mass of sample at depth h, $^{210}Pb_A^0$ is the specific activity at the surface (where h=0), λ is the decay constant of ^{210}Pb (3.11×10^{-2} a^{-1}) and t is the age of the snow sample. Hence:

$$t = \frac{1}{\lambda}\ln\left[\frac{^{210}Pb^0}{^{210}Pb}\right]_A \qquad (8.19.2)$$

Excess unsupported ^{210}Pb occurs in volcanic rocks and arises partly from the radioactive decay of excess ^{226}Ra (half life 1,602 a). A sample from Mount Vesuvius showed enrichment in ^{226}Ra and so in ^{210}Pb also. There is a high ^{210}Pb activity in the mineral cotunnite ($PbCl_2$) which occurs as a sublimate in fumaroles around the volcano and its Pb probably comes from the volcanization of basalts.

^{210}Pb activity in volcanic rocks increases through the radioactive decay of excess ^{226}Ra so that deviations in the $^{210}Pb/^{238}U$ activity ratios cannot simply be put down to elemental fractionation effects in the magma. In the oceans, ^{210}Pb distribution was examined through the GEOSECS Program, particularly in the Pacific. Oceanic boundaries were envisaged as potential sinks in regard to reactive metals in sea water. The ^{210}Pb deficiency relative to its ancestral ^{226}Ra appeared to increase from oceanic interiors towards the continental edges and bottom sea floors where it is more intensively scavenged. Within *ca* 100 m of the latter, a large quantity of excess ^{222}Rn relative to ^{226}Ra has been recorded and attributed to supply by sediments through pore water diffusion. This ^{222}Rn decays to ^{210}Pb and so its effect on the distribution of the latter is manifest. But some vertical profiles in the deep western North Pacific showed no significant variations with depth despite this excess ^{222}Rn. And the apparent box model residence time based on $^{210}Pb/^{222}Rn$ activity ratios decreases from ~100 a in oceanic interiors to 10 a near the bottom. The ^{210}Pb data are explicable using a vertical mixing and first order scavenging model without enhanced scavenging near the sediment-water interface. This indicates that bottom excess ^{222}Rn can scarcely influence ^{210}Pb in the water and that the short residence time mentioned may be an artifact not reflecting the chemical reactivity of Pb. The inference is that the deficiency of ^{210}Pb through scavenging is best estimated using ^{226}Ra not ^{222}Rn. However, the ^{210}Pb scavenging at the sediment-water interface inferred from the oceanic distribution of this radionuclide seems difficult to detect from bottom ^{210}Pb profile measurements.

8.19.4. Thorium-230, uranium-238 and thorium-230, uranium-234

Practically no Th, but. substantial amounts of U are contained in calcium carbonates deposited in saline lakes and in the oceans (where they sometimes reach 5 ppm). Consequently, there is almost no ^{230}Th initial activity in newly deposited carbonates, but, due to the radioactive decay of ^{234}U, the activity of the former increases with time and the following expression can be presented:

$$^{230}Th_{Ax} = {}^{230}Th_x\lambda_{230} = \frac{\lambda_{230}}{\lambda_{230}-\lambda_{234}}\,{}^{234}U^{o}_{As}\left[e^{-}\lambda_{243}t - e\,\lambda_{230}t\right]$$

and the excess activity of the ^{234}U is:

$$^{234}U^{o}_{Ax} = {}^{234}\,U^{o}_{z} - {}^{234}\,U_{As}$$

where $^{234}U^{o}_{Ax}$ is the total initial activity of excess ^{234}U when deposition occurred and $^{234}U_{As}$ is the activity of ^{234}U which is in secular equilibrium with ^{238}U, t = time and λ = relevant decay constant. As a consequence:

$$^{230}Th_{Ax} = \frac{\lambda_{230}}{\lambda_{230}-\lambda_{234}}\left({}^{234}U^{o}_{A} - {}^{234}\,U^{o}_{As}\right)\left(e^{-}\lambda_{234}t - e^{-}\lambda_{230}t\right)$$

and the activity of $^{230}Th_{Ax}$ relative to ^{238}U is:

$$\left[\frac{^{230}Th}{^{238}U}\right]_{Ax} = \frac{\lambda_{230}}{\lambda_{230}-\lambda_{234}}\left[\frac{^{234}U^{o}_{A} - {}^{234}\,U_{As}}{^{238}U_{A}}\right]\left(e^{-\lambda}234^{t} - e^{-\lambda}230^{t}\right)$$

The method has been used to date corals, e.g. from the 3 lowest terraces of Barbados which is an island apparently emerging from the sea at a uniform rate [54]. Data from the $^{230}Th/^{234}U$ activity ratios of coral samples gave dates of 122,000, 103,000 and 82,000 a. These coincide with predicted times of elevated summer radiation at 45 °N latitude [55]. A suitable equation for dating both corals and molluscs as well as calcareous oozes follows:

$$\left[\frac{^{230}Th}{^{238}U}\right]_{A} = \left(1 - e^{-}\lambda_{230}t + \frac{\lambda_{230}}{\lambda_{230}-\lambda_{234}}\left(\gamma_{o}-1\right)\left(e^{-\lambda}234^{t} - e^{-\lambda}230^{t}\right)\right)$$

where $\gamma_o = {}^{234}U^{o}_{A}\,/^{238}\,U_A$ and $^{234}U_{As} = {}^{238}U_A$. Certain conditions must apply. Firstly the initial activity ratio must be close to zero. Secondly the sample must have been a closed system as

regards U and intermediates between ^{238}U and ^{230}Th. Thirdly the initial activity ratio $[^{234}U/^{238}U]^0_A$ must be known. Of course, it is possible to relate the activity of ^{230}Th to that of its immediate parent, ^{234}U, since, if the ^{234}U is in secular equilibrium with ^{238}U, then the $[^{230}Th/^{234}U]_A$ activity ratio is related to time, *t*, thus:

$$\left[\frac{^{230}Th}{^{234}U}\right]_A = 1 - e^{-}\lambda_{230}t$$

although this does not take into account the possible presence of excess ^{234}U. In cases where γ_o=>1, the $[^{230}Th/^{238}U]$ activity ratio as a function of time is obtainable by combining the last equation with the last one given below in section 16.5 (the $^{234}U/^{238}U$ geochronometer). However, this may not be necessary. It seems likely that the presence of such excess ^{234}U may make little difference to the observed $[^{230}Th/^{234}U]_A$ activity ratios of marine carbonates. Thus, using the last equation above gave over-estimates of only *ca* 2% for samples which are 130,000 a old.

8.19.5. The uranium-234, uranium-238 geochronometer

Attainment of secular equilibrium in radioactive decay series starting with ^{238}U, ^{235}U and ^{232}Th depends on none of the relevant daughters leaving or entering the systems concerned. Once the equilibrium is established, the decay rates of the daughters in any particular system equal that of the parent:

$$\lambda_1 N_1 = \lambda_2 N_2 = \lambda_3 N_3 = \ldots\ldots \lambda_n N_n$$

where $\lambda_1 N_1$ is the radioactive decay rate of the parent and the other terms represent those of the daughters. Under secular equilibrium conditions, the ratio between the decay rate of any daughter and its parent is equal to 1. The production of ^{234}U from its parent proceeds as follows:

$$^{238}U \xrightarrow{\alpha} {}^{234}Th \xrightarrow{\beta^-} {}^{234}Pa \xrightarrow{\beta^-} {}^{234}U$$

so that, where secular equilibrium obtains, the rate of decay of ^{234}U in an uranium-bearing mineral equals that of ^{238}U and the activity ratio $[^{234}U/^{238}U]_A$=1. However, groundwater samples show that such secular equilibrium does not exist and was also absent from minerals deposited from it [56]. In fact, the value of the ratio usually exceeds 1 because the ^{234}U is enriched by processes such as the radioactive decay of its parent dissolved in groundwater. This alpha decay damages the crystal lattice and allows the daughter to migrate through micro-capillaries in the mineral and oxidize to form uranyl ions which dissolve in water and remove it into an aqueous phase. ^{238}U occurs in stable lattice positions. ^{234}Th can be rejected from grain surfaces through the recoil in alpha-decay of the radionuclide then decaying to ^{234}U via the short lived ^{234}Pa. In general, activity ratios $[^{234}U/^{238}U]_A$ both in surface and groundwaters as well as in secondary minerals containing U on continents, normally exceed 1 and can reach values as high as 10. But the activity ratios of primary U minerals in rocks which have been chemically weathered may be less than 1 through the preferential removal of ^{234}U. If U occurs in solution in groundwater, it may enter oceans and become isotopically homogenized, the relevant activity ratio, $[^{234}U/^{238}U]$ having a narrow spread of values with a mean of *ca* 1.15. The element can be removed from oceans by incorporation into authigenic minerals, e.g. $CaCO_3$, or by adsorption on to surfaces of grains under reducing conditions. Once U has been isolated from sea water, ^{234}U decays to ^{230}Th until the activity ratio, $[^{234}U/^{238}U]_A$, approaches an equilibrium value. But it is not possible to use this as a dating method because of the chance that ^{234}U migrated after deposition. However, the radioactive decay of excess ^{234}U and the growth of its daughter ^{230}Th have been used for the dating of marine and non-marine carbonates of Pleistocene age.

If $^{234}U_A$ be the activity of this radioisotope per unit mass of sample now, $^{234}U_{As}$ the specific activity of its secular equilibrium with ^{238}U and $^{234}U_{Ax}$ the activity of excess ^{234}U per unit mass of sample, then:

$$^{234}U_A = {}^{234}U_{As} + {}^{234}U_{Ax}$$

and the activity of the excess ^{234}U will diminish as a function of time, *t*:

$$^{234}U_{Ax} = {}^{234}U^{o}_{Ax}\, e^{-\lambda_{234} t}$$

where the first term is the initial specific activity of the excess ^{234}U expressible as:

$$^{234}U_{Ax} = {}^{234}U^{o}_{A} - {}^{234}U_{As}$$

where $^{234}U^{o}_{A}$ is the total initial activity of ^{234}U and $^{234}U_{As}$ is the component supported by ^{238}U. Since $^{234}U_{As}=^{238}U_{A}$, a combined equation can be derived:

$$^{234}U_{A} = {}^{238}U_{A} + ({}^{234}U^{o}_{A} - {}^{238}U_{A})e^{-\lambda_{234} t}$$

and dividing this by the constant specific activity of ^{238}U gives:

$$\left[\frac{^{234}U}{^{238}U}\right]_{A} = 1 + \left[\frac{^{234}U^{o}_{A} - {}^{238}U_{A}}{^{238}U_{A}}\right] e^{-\lambda_{234} t}$$

and then:

$$\left[\frac{^{243}U}{^{238}U}\right]_{A} = 1 + (\gamma_{o} - 1)e^{-\lambda_{234} t}$$

γ_0 being the initial$[^{234}U/^{238}U]^{0}_{A}$ ration of the sample.

The geochronometer so derived involves a determination for γ_o=1.15 and was applied to dating the $CaCO_3$ of biogenic and inorganic origin deposited both in marine and non-marine environments. But the reliability of ages from the latter is restricted by uncertainty regarding the value of γ_o. In non-marine areas, this factor shows time-dependent variations since shells of some non-marine molluscs actually acquire U after the death of the organisms. However, since groundwater can enrich in ^{238}U relative to its parent, this enables its specific sources to be assessed. Also, the mixing of different water masses characterized by their individual $[^{234}U/^{238}U]_{A}$ activity ratios can be determined [57].

8.20. URANIUM/THORIUM/LEAD

8.20.1. Radioactive decay series

After radioactivity was identified in U and Th minerals, it was used to date them and methods included Pb/U, Pb/alpha, U/He, U/Th/Pb and common Pb of which the last two are still utilized. Natural U comprises 99.28% ^{238}U (half life 4.5×10^{9} a), 0.71% ^{235}U (half life 7.1×10^{8} a) and 0.006% ^{234}U (half life 2.5×10^{5} a). The common radioactive isotope of Th is ^{232}Th (half life 1.4×10^{10} a) and its relative abundance in nature is 100%. From the above data, the corresponding decay constants of these primordial radio nuclides may be derived and they are as follows:

^{238}U: 1.55125×10^{-10} a^{-1}
^{235}U: 9.8485×10^{-10} a^{-1}
^{234}U: 2.806×10^{-6} a^{-1}
^{232}Th: 4.948×10^{-11} a^{-1}

All have α-decay modes. In the case of U, ^{238}U and ^{235}U can exist in meta-stable states and emit γ-quanta due to isomeric decay to the ground states. With ^{232}Th, it has an intermediate radioactive daughter, ^{228}Th, with a half life of 1,913 a. ^{238}U also has daughters, namely ^{234}Th (half life 24.1 d) and ^{230}Th (half life 7.54×10^{4} a), which are insignificant. The radioactive decay of ^{238}U initiates the uranium series ($A=4n+2$, v. accompanying Figure 8.20.1) which includes ^{234}U as a daughter and ends in stable ^{206}Pb. The series may be expressed as follows:

$$^{238}U \rightarrow {}^{206}Pb + 8{}^{4}He + 6\beta^{-1} + Q$$

where Q=47.4 MeV atom^{-1}. Each atom of ^{238}U undergoing radioactive decay produces eventually one atom of ^{206}Pb as a result of the cumulative emissions of 8 α-particles and 6 negatrons. This presumes that the decay occurred in a closed system regarding U, Pb and all intermediate daughters and Q represents all the decay energies of the series. Some intermediate daughters undergo branched decay entailing emissions of either α-particles or negatrons. However, stable ^{206}Pb remains the end product of all possible decay paths.

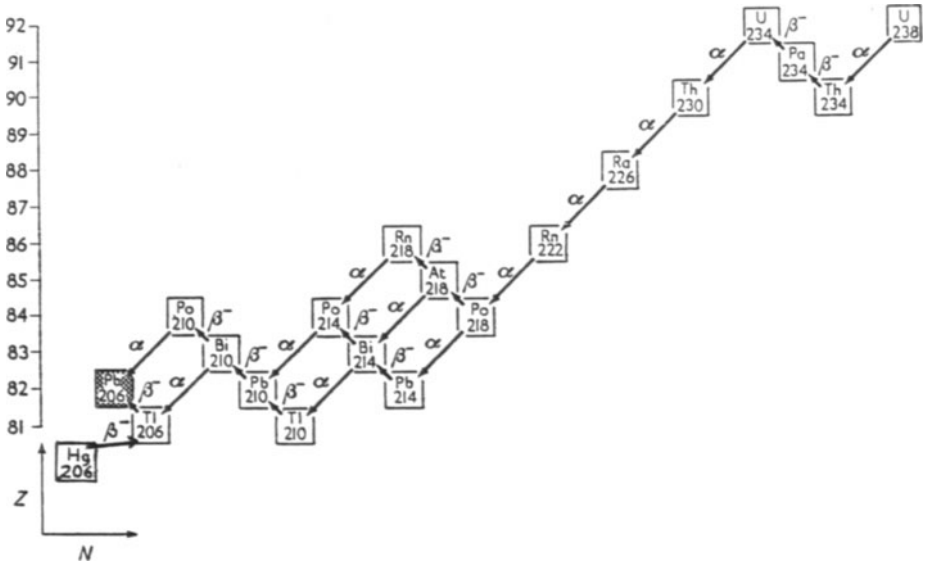

Figure 8.20.1. The ^{238}U (uranium) family ($A = 4n + 2$) radioactive decay sequence.

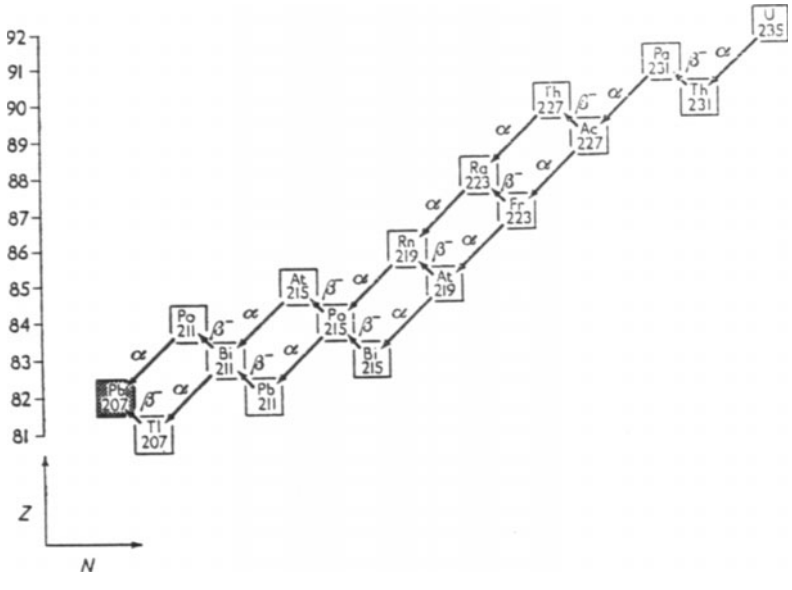

Figure 8.20.2. The ^{235}U (actinium) family ($4n + 3$) radioactive decay sequence.

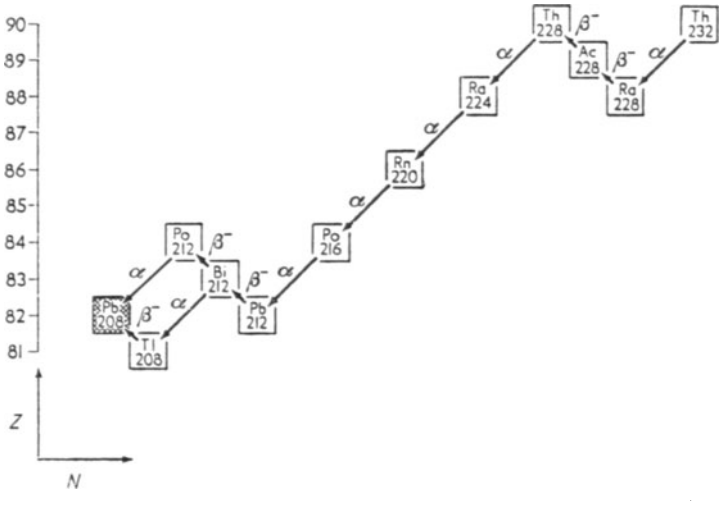

Figure 8.20.3. The ^{232}Th (thorium) family ($4n$) radioactive decay sequence.

The radioactive decay of ^{235}U produces stable ^{207}Pb after the emission of 7 α-particles and 4 negatrons and constitutes the actinium series (A=$4n$+3), *v.* accompanying Figure 8.20.2. The process may be represented as follows:

$$^{235}\text{U} \rightarrow {}^{207}\text{Pb} + 7{}^{4}\text{He} + 4\beta^{-1} + Q$$

where Q=45.2 MeV atom^{-1}.

The radioactive decay of ^{232}Th produces stable ^{208}Pb after the emission of 6 α-particles and 4 negatrons and constitutes the thorium series (A=$4n$), v. accompanying Figure 8.20.3. The process may be represented as follows:

$$^{232}\text{Th} \rightarrow {}^{208}\text{Pb} + 6{}^{4}\text{He} + 4\beta^{-1} + Q$$

where Q=39.8 MeV atom^{-1}. Branched decay again occurs.

Altogether, 42 isotopes of 12 elements are formed as intermediate daughters in the 3 decay series, but none is a member of more than one series so that each of the series terminates in specific isotopes of Pb. The half lives of the respective parents are longer by orders of magnitude than those of the various daughters, hence the decay series fulfil the requirements for the establishment of secular equilibrium and the decay rates of the intermediate daughters are equal to those of their respective parents.

If the mineral used is a closed system and such a secular equilibrium exists, the rate of production of the stable daughter at the end of a particular decay series is equal to the rate of decay of the relevant parent. Therefore it is feasible to regard the radioactive decay of the U and Th isotopes in minerals as if it went directly to the respective Pb isotopes. This simplifies the equations required to describe the growth of radiogenic Pb in uranium- and thorium-bearing minerals.

There are 4 naturally occurring isotopes of Pb, namely ^{204}Pb, ^{206}Pb, ^{207}Pb and ^{208}Pb, the total number for the element being 32 and the remaining 28 being radioactive and extremely short lived. Actually ^{204}Pb is also very slightly radioactive, but can be regarded as stable because of its enormously long half life of 1.4×10^{17} a. The relative abundances of the 4 significant isotopes of Pb are 52.4% for ^{208}Pb, 22.1% for ^{207}Pb, 24.1% for ^{206}Pb and 1.4% for ^{204}Pb.

The following equations express the isotopic composition of Pb in uranium- and thorium-bearing minerals:

$$\frac{^{206}Pb}{^{204}Pb} = \left[\frac{^{206}Pb}{^{204}Pb}\right]_i + \frac{^{238}U}{^{204}Pb}\left(e^{\lambda_1 t} - 1\right)$$

$$\frac{^{207}Pb}{^{204}Pb} = \left[\frac{^{207}Pb}{^{204}Pb}\right]_i + \frac{^{235}U}{^{204}Pb}\left(e^{\lambda_2 t} - 1\right)$$

$$\frac{^{208}Pb}{^{204}Pb} = \left[\frac{^{208}Pb}{^{204}Pb}\right]_i + \frac{^{232}Th}{^{204}Pb}\left(e^{\lambda_3 t} - 1\right)$$

where the first terms are measured data from the mineral samples, those with the subscript i are the initial ratios when the Pb was incorporated into the minerals during crystallization, the U and Th ratios to the relevant Pb isotopes are measured and λ_1, λ_2 and λ_3 are the respective decay constants of ^{238}U, ^{235}U and ^{232}Th respectively while t is the time elapsed since the mineral samples closed to U, Th, Pb and all intermediate daughters. Isotope dilution can be used to date uranium- and thorium-bearing minerals and to ascertain the concentrations of these elements. The isotopic composition of Pb may be determined using mass spectrometry. The equation for finding t in a in the case of ^{238}U is as follows:

$$t_{206} = \frac{1}{\lambda_1}\ln\left[\frac{\frac{^{206}Pb}{^{204}Pb} - \left[\frac{^{206}Pb}{^{204}Pb}\right]_i}{\frac{^{238}U}{^{204}Pb}}\right] + 1 \qquad (8.20.1)$$

and similar equation exist for ^{235}U and ^{232}Th. Results embody 3 independent ages referring to the 3 decay series involved and ideally should agree, but will do so only if the mineral samples analyzed stayed closed throughout their geological history, and the isotopic composition of U and Th was not modified in any way, e.g. by isotopic fractionation. It is assumed that the values used for the initial Pb isotope ratios are accurate and that no analytical or systematic errors occurred. If discordant dates are obtained, as often happens, the inference is that the mineral samples concerned did not survive closed through geological time after crystallization. However, corrections can be made to the data, for instance if Pb was lost, the effect on U/Pb dates can be minimized by calculating a date based on the $^{207}Pb/^{206}Pb$ ratio which is not sensitive to such loss. Minimum sensitivity is shown where the loss was recent and when the Pb lost had the same isotopic composition as the residual Pb, i.e. isotopic fractionation did not occur. An appropriate equation is as follows:

$$\frac{\frac{^{207}Pb}{^{204}Pb} - \left[\frac{^{207}Pb}{^{204}Pb}\right]_i}{\frac{^{206}Pb}{^{204}Pb} - \left[\frac{^{206}Pb}{^{204}Pb}\right]_i} = \frac{^{235}U}{^{238}U}\left[\frac{e^{\lambda_2 t} - 1}{e^{\lambda_1 t} - 1}\right]$$

the ratio $^{235}U/^{238}U$ being 1/137.88 for U of normal composition found in terrestrial minerals, lunar rocks and meteorites. Hence it is possible to obtain a "207–206" date without any knowledge of the U concentration in the mineral concerned. Thus the above equation may be amended by substituting the ratio $^{207}Pb/^{206}Pb$ for the right hand side. Tables exist from which t may be interpolated for any desired value of this ratio. At present, t=0 and the ratio = 0.04607. This equals that of the radioactive decay rates of the parents and is minimal in accordance with the low relative abundance of ^{235}U in U (0.72%).

Although U and Th occur in many minerals, only a few of these are suitable for dating by means of the U, Th–Pb approach. They comprise those which can retain these elements adequately and probably the most retentive mineral is zircon. In sedimentary rocks, zircon derived from sources underlaid by igneous-metamorphic complexes will embody a record of the orogenic and magmatic histories of the said sources. In zircons, the concentrations of U and Th average 1,330 and 560 ppm, respectively, but in pegmatites greater concentrations occur. U and Th are present in zircons through the isomorphous replacement of Zr^{4+} (ionic radius 0.087 nm) by U^{4+} (1.05 nm) and Th^{4+} (0.11 nm), also through the presence of thorite inclusions. Such substitution is restricted by the differences in the relevant ionic radii and Pb^{2+} is excluded altogether because its ionic radius is 0.132 nm. In addition, it carries a lower charge. Hence zircon does not contain much Pb when it crystallizes and has very high ratios for U/Pb and Th/Pb which makes it an invaluable geochronometer. Hydrothermal decomposition in a sealed pressure vessel has been utilized in order to extract Pb and U from zircons.

8.20.2. Concordia and discordia

The concept of two independent geochronometers arose from consideration of the radioactive decay of the naturally occurring radioisotopes of U, ^{238}U and ^{235}U. For the former, this is expressible as follows:

$$\left(\frac{^{206}Pb}{^{238}U}\right)_x = e^{\lambda_1 t} - 1$$

where:

$$\left(\frac{^{206}Pb}{^{238}U}\right)_x = \frac{\dfrac{^{206}Pb}{^{204}Pb} - \left[\dfrac{^{206}Pb}{^{204}Pb}\right]_i}{\dfrac{^{238}U}{^{204}Pb}}$$

and the other decay series can be treated similarly. Such equations give concordant dates if an uranium-bearing mineral is analyzed which satisfies the required assumptions regarding closed systems. The above and the equivalents for the actinium series (from ^{235}U to ^{207}Pb) constitute the parametric equations of a particular curve representing the loci of all concordant U/Pb systems, this curve being termed the concordia. It is such that $t\,(^{206}Pb/^{238}U) = t\,(^{207}Pb/^{235}U)$ and all samples having concordant dates must plot on this curve. Those which do not exemplify episodic Pb loss. If all radiogenic Pb accumulated up to such a Pb loss episode is lost during that episode, the system responds in such a manner that those coordinate points which represent it return to the origin and the U/Pb geochronometer recommences, i.e. the geological "clock" is reset. Of course, when this happens, all trace of the earlier geological histrory of the relevant system disappears. If only some radiogenic Pb is lost, points move part way along a chord comprising systems with discordant dates, in other words a discordia. The accompanying Figure 8.20.4 constitutes a concordia diagram.

Concordia diagrams permit interpretation of the geological histories of U–Pb systems and provide information regarding past disturbances of these systems. Several concordia models have been developed in order to interpret the discordancy of the U/Pb dates of uranium-bearing minerals. One is the dilatancy model [58]. Minerals undergo radiation damage through the alpha-decay of U, Th and their daughters and the extent of this increases with increasing age as well as with the U and Th contents of the relevant minerals. Such damage is responsible for micro-capillaries allowing water to enter crystals. This is retained until uplift and erosion releases the pressure on minerals, such consequent dilatance of zircons being accompanied by the escape of water and dissolved radiogenic Pb. This loss of radiogenic Pb probably took place during the uplift and erosion of crystalline basement complexes in Precambrian shields. Researches have shown that 207–206 dates from these frequently approximate the true ages of uranium-bearing minerals. Such minerals from different continents may have lost radiogenic Pb 500 Ma to 600 Ma ago as a result

of the Pan-African Event and parallel happenings in other parts of Gondwana such as the Brazilian Event.

A second model is based on chemical weathering which affects practically all rocks and minerals which outcrop and a third model is a continuous diffusion one in which radiogenic Pb diffused from crystals at a rate governed by a diffusion coefficient, D, an effective radius, a, and a concentration gradient of $^{206}Pb/^{238}U$ (ordinate) against $^{207}Pb/^{235}U$ (abscissa). The crystals are assumed to be spherical and it is assumed also that there has been no or negligible diffusion of U and intermediates. It is assumed too that the radiogenic Pb diffusion followed Fick's Law. The following expression refers to the change in Pb concentration with time for any radial volume element in a sphere:

$$\frac{\partial C}{\partial t} = D\frac{\partial^2 C}{\partial^2 r} + \frac{2}{r}\frac{\partial C}{\partial r} + N_0 e^{-\lambda t}$$

where C is the atom concentration of Pb daughter, N_0 is the initial concentration of U parental atoms, λ is the decay constant of the parent U and t is the time elapsed since crystallization occurred. The relevant boundary conditions are $C=0$, $t=0$.

It is possible to plot isochrons in coordinates of $^{206}Pb/^{204}Pb$ and $^{238}U/^{208}Pb$ and similar ones can be constructed for $^{235}U/^{207}Pb$ and $^{232}Th/^{208}Pb$ as well. Three isochrons result and their slopes indicate the age of the suite of samples analyzed, if these came from closed systems having identical initial Pb isotope ratios. Such isochrons have been used to date samples of granite from the USA, Australia and the former USSR.

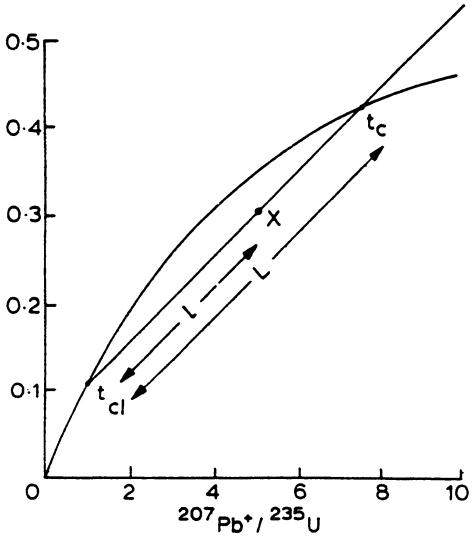

Figure 8.20.4. Concordia diagram showing the effects of Pb loss and U gain or loss on U/Pb systems. t_c = time elapsed since original crystallization, t_{c1} = time elapsed since closure of the system after Pb loss or U gain.

8.20.3. Common lead and the Holmes/Houtermans model

Common Pb is found in many minerals, e.g. galena, PbS, and cerussite, $PbCO_3$, which are constituents of ore-forming bodies. In addition, it occurs as a trace element in minerals where associated U and Th contents are low as well as in rock-forming minerals such as feldspars (in K feldspar, Pb^{2+} can replace K^+). It has long been recognized that the atomic weight of ordinary Pb^{2+} is less than that of common Pb associated with U and the difference is due to the presence of radiogenic ^{206}Pb. Common Pb contains isotopes of Pb with mass numbers 204, 206, 207 and 208, the first of these not being the decay product of a radioactive series and the others originating with

the radioactive series initiated by ^{238}U, ^{235}U and ^{232}Th respectively. Amounts of these three may be related to that of ^{204}Pb and the atom number ratio described as follows:

$$\alpha = {}^{206}Pb/{}^{204}Pb, \beta = {}^{207}Pb/{}^{204}Pb, \gamma = {}^{208}Pb/{}^{204}Pb$$

Every lead contains a measurable quantity of ^{204}Pb and may be represented in a three-dimensional diagram of the variables α, β and γ. As early as the late 1930s, it was discovered that large variations in the isotopic composition of common Pb from different sources existed and at first this was difficult to understand because prior observations had implied that common Pb had a constant average atomic mass. However, it soon became clear that this supposed constancy was fortuitous, reflecting the fact that the increase in the $^{206}Pb/^{204}Pb$ ratios is often accompanied by a comparable rise in the $^{208}Pb/^{204}Pb$ ratio.

Efforts have been made to construct quantitative models for the isotopic evolution of Pb in the Earth from which the age of the planet and also that of common Pb could be derived. Independently, two were made in 1946 by Arthur Holmes and F. G. Houtermans [59,60]. They supposed that the Earth was originally both fluid and homogeneous with U, Th and Pb uniformly distributed and with primaeval Pb having the same isotopic composition everywhere. Later, the Earth was thought to have rigidified so that small regional differences in the U/Pb ratio arose. In any given region, this ratio was believed to have changed solely due to the radioactive decay of U to Pb. It was also assumed that, when a common Pb mineral crystallized, the Pb separated from U and Th with its isotopic composition thereafter remaining constant. The Holmes/Houtermans model facilitated understanding differences in α, β and γ for various types of common Pb and allowed calculation to be made of the time elapsed since the formation of the Earth's crust and the time at which common Pb became incorporated into an ore. Most of the Pb in the accessible parts of the crust occurs in igneous and sedimentary rocks with a content of from a few tenths to say 50 ppm of Pb. Only a tiny proportion of crustal Pb is in minerals or ore bodies comprising more than 0.1% of Pb and this is true for crustal U and Th as well. So the incorporation of Pb into a Pb mineral is a very rare event from which it may be inferred that the probability of the event occurring twice in the history of any given sample of Pb is negligible.

In the source rock from which a given sample of common Pb is obtained due to mineralization or ore formation processes, Pb was connected to given amounts of U and Th. This can be described by using a chemical milieu index, μ, the atom number of ^{238}U over ^{204}Pb comprising the milieu from which the sample of common Pb came. As the ^{238}U decays with time, the content may be extrapolated to the present as if the original mother rock still existed. The chemical milieu index may be defined as follows:

$$\mu = {}^{238}U_{today}/{}^{204}Pb_{today}$$

Similarly it is possible to define another chemical milieu index for the mother rock of a given sample of common Pb by means of the ratio between the number of atoms of ^{232}Th and the atom number of ^{238}U extrapolated to the present day and the following is applicable to this index, x,

$$x = {}^{232}Th_{today}/{}^{238}U_{today}$$

The Holmes/Houtermans model assumed that all common Pb has an isotopic composition explicable by the adding of radiogenic Pb as decay products from ^{238}U, ^{235}U and ^{232}Th associated with a primaeval Pb at the time of formation of the Earth. This primaeval Pb is characterized by the relative isotope abundances α_w, β_w and γ_w, where w is the age of the Earth. It is taken for granted that the chemical milieu indices for a given sample of common Pb stayed constant from w to a time p, where p is the time elapsed since a given sample of Pb became incorporated into a Pb mineral to which, therefore, a model age of p may be assigned). From the general equation of radioactive decay, it is clear that a sample of Pb has changed its isotopic composition only by the addition of the isotopes ^{206}Pb, ^{207}Pb and ^{208}Pb from U and Th with which it was linked in the mother rock during the time interval w–p. Expanding mathematically, it proved possible to obtain a value for the age of the Earth which was $w \cong 3 \times 10^9$ a.

A further impetus to research came from the investigation of the isotope composition of minute quantities of Pb in iron meteorites, particularly in the iron and troilite phases of Cañon Diablo. The α and β values turned out to be far lower than those from samples of terrestrial Pb or Pb from

stony meteorites. The troilite (FeS) phase, while containing Pb, does not contain U and Th, hence the isotopic composition of the Pb was regarded as practically constant since crystallization. Such Pb is the least radiogenic available and may approach primaeval Pb in isotopic composition. In fact, the Canon Diablo Pb values may approximate that of primaeval Pb initially indorporated into the Earth's crust and also into chondritic material. If these values are assumed for α_w and β_w, and taking the isotopic compositions of a number of rather recent leads or values measured from young leads from oceanic manganeses nodules into account, w may be calculated as 4.5±0.05 Ga. All models of this type for the isotopic change with time from the formation of the Earth's crust up to a time p of mineralization involve the hypothesis that the Pb spent the entire time interval $(w - p)$ in a milieu having a constant value of μ. It is interesting that phenomena such as metamorphism which occurred often during Earth history do not seem to have influenced the μ-values of the mother material of Pb minerals to any great extent. However, there is a small dispersion in the x-values. The Holmes/Houtermans model is shown in the accompanying Figure 8.20.5. Serious problems with the Holmes/Houtermans model arose from anomalous Pb as opposed to common Pb which yield meaningful model dates. It is likely that the small number of ore deposits with ordinary Pb reflects the fact that Pb in most of these underwent a more complex history than that envisaged in the Holmes/Houtermans model. To conform with this model, the relevant Pb must have had a single stage history and this can be confirmed if the.model dates agree reasonably well with isotopic dates obtained from other minerals from the ore and if the isotopic ratios of Pb from a particular deposit are constant within experimental error.

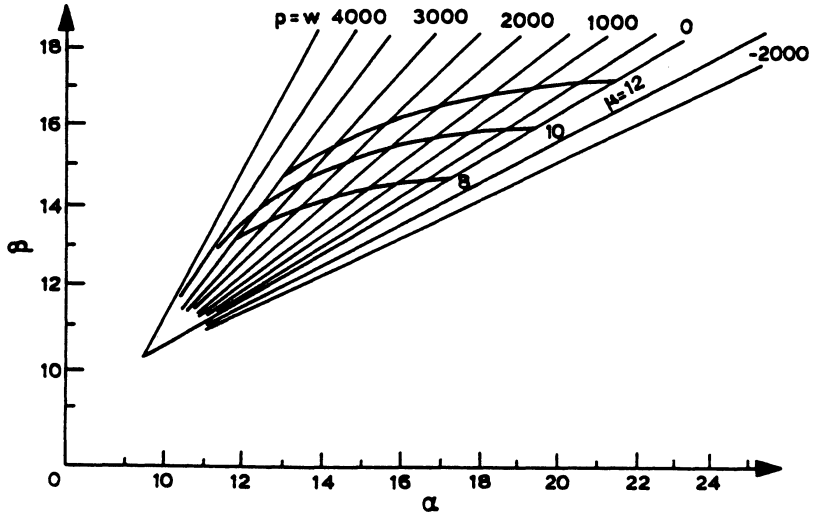

Figure 8.20.5. This is a graphic presentation of the Holmes/Houtermans model for common Pb (Berne data). The straight lines are isochrons, the curved lines are Pb development lines. The relevant constants are as follows:
α_w=9.41, β_w=10.27, γ_w=29.2, w=4.49 Ga, ε=1/139, λ_1=1.54×10^{-4} Ma^{-1}, λ_2=9.80×10^{-4} Ma^{-1}.
The point α_w, β_w represents primaeval Pb and from it emerge several curved lines given by the following equations:
$a-a_w=\mu\varepsilon(e^{\lambda_1 w}-e^{\lambda_1 p})$
$b-b_w=\mu\varepsilon(e^{\lambda_1 w}-e^{\lambda_1 p})$
where $\varepsilon = (^{235}U)_{today}/(^{238}U)_{today}$.
Dividing the penultimate equation by the last one above, the "lead-lead" age of extra Pb accumulated by a given sample of primaeval Pb with which it was associated during the time interval $(w - p)$ can be represented as follows:

$$\frac{\beta - \beta_w}{\alpha - \alpha_w} = \varepsilon \cdot \frac{e^{\lambda' w} - e^{\lambda' p}}{e^{\lambda w} - e^{\lambda p}}$$

and this eliminates any necessity to involve the constant μ. This leaves only 4 constants to be assessed, i.e. α_w, β_w, γ_w and p. Hence, from 3 pairs of α and β of known age p, of which 2 p-values may be equal, the values for α_w and β_w can be extrapolated and the age of the Eerth, w, evaluated. A first statement of $\gamma-\gamma_w = x\mu(e^{\lambda'' w} - e^{\lambda'' p})$ but as noted μ may now be neglected.

8.20.4. Anomalous leads

The basic premise as regards the development of the isotopic composition of Pb is the addition of radiogenic isotopes ^{206}Pb, ^{207}Pb and ^{208}Pb from the radioactive decay of U and Th with values of μ and $x\mu$ which remained constant during the time interval $(w - p)$. Unfortunately, p does not always coincide with the time of mineralization as was shown by fossils in beds containing veins of Pb ore. Indeed, absurd results have been obtained which led to negative ages so that common Pb ores existing now should form in the far future (up to 2 Ga later).*

Two types of anomaly are termed B and J. The former are those in which the model age p may exceed the geological age of the rock containing the Pb ores and is named after Bleiberg in Austria. Causes include pneumatolysis which can redistribute Pb minerals in ore bodies or veins and so produce a condition where $g < p$, g being the geological age.

J-type anomalies were so called after Pbs such as those of Joplin, Sudbury, Ontario, Canada and, for them, applying the Holmes/Houtermans model equation gave negative model ages. However, there are instances of apparently normal Pbs belonging to this type and giving model ages more or less inferior to the age of mineralization. These are difficult to recognize, but sometimes can be identified through their anomalous x–values. Explaining J-type anomalies is straightforward, bearing in mind that a basic assumption of the model is that μ had a constant value during the time interval $(w - p)$. Clearly, this cannot be more than, at best, a first approximation of the actual history of a Pb sample. Thus, if purely common Pb were mixed with a small quantity of radiogenic Pb, an isotopic composition would result which would resemble a J-type anomalous Pb. And such an event could occur in nature at any time during the time interval $(w - p)$ before the uranium- and thorium-contents of the Pb sample dropped to zero.

A single analysis of an anomalous Pb of J-type gives little information about the date when radiogenic Pb was added between w and p or about the isotopic composition and hence the age. Better data are obtained from many samples in a region. Three case histories were offered for three different regions containing Pb ore deposits, namely Sudbury and Thunder Bay, Ontario, and Australia. Common Pbs and highly anomalous Pbs were involved, the former following a Pb development line without appreciable alteration in their μ- and x-values during the time interval $(w - p)$. They have model ages corresponding to the actual time of mineralization [61]. Of course, the isotopic data alone do not suffice to determine the time of addition of the radiogenic component of such anomalous J-type Pbs.

Alternatives to the Holmes/Houtermans model have been proposed. The Russell/Standton/ /Farquhsar (RSF) and the Russell/Farquhar/Cumming (RFC) models were based on work by others [62]. While the Holmes/Houtermans model presented a fan of Pb development lines and isochrons starting at a point corresponding to primaeval Pb (α_w, β_w) or a similar α,γ-diagram, both of the others assumed a single global source material for all "ordinary" common leads which could be in the upper mantle. cf. Figure 8.20.5. A continuous growth model has been suggested and considered as more feasible since it is likelier that radiogenic contaminants were generated continuously during a time interval starting with the formation of the relevant rocks, e.g. granites, and ending with the removal of radiogenic Pb from them to mix with other Pb prior to or in the course of formation of a Pb ore deposit.

8.20.5. Multistage leads

Leads in igneous and metamorphic rocks have isotopic compositions determined by a multistage history in most cases. Thus it is clear that they will have had past associations with a number of systems possessing different U/Pb and Th/Pb ratios. In the complex situation of a sample of Pb which at a point p has undergone transference through two uranium-bearing systems characterized by different $^{238}U/^{204}Pb$ ratios designated as μ_1 and μ_2 the α-value of the sample is given by:

$$\alpha = \alpha_w + \mu_1\left(e^{\lambda_1 w} - e^{\lambda_1 p}\right) + \mu_2\left(e^{\lambda_1 p_1} - e^{\lambda_1 p_2}\right)$$

*Douglas Adams's *The Hitchhiker's Guide to the Galaxy* may turn out to have some scientific background after all (the editors).

and, when Pb is transferred from the first system to the second, this probably entails a physical process of removal, e.g. through the formation of magma in the mantle and its later emplacement in the crust of the Earth. It is also possible that such a transition from system 1 to system 2 might occur without such a physical removal, i.e. take place solely through changes in the U/Pb system of system 1. These would affect the $^{238}U/^{204}Pb$ ratio and so the isotopic composition of the Pb which became incorporated into an ore deposit. A rarer possibility is that Pb may be gained and its different isotopic composition would alter the isotopic composition of the final Pb. It is clear that all of the above considerations would apply to three or more stages as well.

8.20.6. Whole rock dating

Considering Pb-Pb isochrons of igneous and metamorphic rocks, if a magma volume involving homogeneous material crystallizes a rock suite results which contains different U/Pb and Th/Pb ratios. Alternatively, a volcanic rock assemblage might arise after a high grade regional metamorphic episode and contain Pb isotopically homogenized by the event. Either way, the Pb later evolved along a set of divergent and curved trajectories corresponding to different values of μ in each specimen. If such growth proceeds to the present time uninterruptedly, the Pbs lie along an isochron if the rocks had the same initial istitope.ratios of Pb formed at the same time and remained closed to U, Th and Pb. Recent alterations in the concentrations of these elements are permissible if the isotopic composition of the Pb is unaffected. An isochron equation can be derived of which the slope is given by:

$$S = \frac{1}{137.88}\frac{\left(e^{\lambda_2 t} - 1\right)}{\left(e^{\lambda_1 t} - 1\right)}$$

where S is the slope. From this, the age of a suite of samples can be obtained. One application may be cited [58]. A suite of metamorphic rocks from the Lewisian basement complex in northwestern Scotland was depleted in U compared with the crustal average. U and Pb concentrations were given as 0.24 and 7.9 ppm, respectively, and the average $^{238}U/^{204}Pb$ ratio was 1.76. The isotope ratios of Pb scattered about a straight line interpreted as a secondary isochron. A date was found from the point of intersection of this with the primary Pb growth curve which had a value of 8.68 for μ, near to, but lower than the value for conformable Pb ores. The result was an age of *ca* 2.9 Ga which was taken to be the time of variable U loss during pyroxene-granulite metamorphism of the ancestral Lewisian rocks.

8.21. URANIUM/XENON, URANIUM/KRYPTON

U undergoes spontaneous fission as well as radioactive α-decay and this produces fissiogenic Xe and Kr which accumulate in uranium-bearing minerals through geological time. The proposal to use these for determining the age of such minerals was made as early as 1947 when Khlopin et al [63] discovered Xe produced by the spontaneous fission of ^{238}U in pitchblende. MacNamara and Thode [64] were the first to give the isotopic compositions of Xe_{sf} and Kr_{sf}. An U/Xe or U/Kr age can be calculated as follows:

$$t_{(U/Xe)} = \frac{1}{\lambda_\alpha + \lambda_{sf}} \ln\left[\frac{{}^{A}Xe_{sf}\left(\lambda_\alpha + \lambda_{sf}\right)}{{}^{238}U^{i}Y_{sf}\lambda_{sf}} + 1\right]$$

where λ_α is the α-decay constant of ^{238}U, λ_{sf} is the ^{238}U spontaneous fission decay constant and ${}^{A}Xe_{sf}$ and ${}^{A}Y_{sf}$ are concentration and mass yield, respectively, for a Xe or Kr isotope with a mass number A resulting from spontaneous fission. Eikenberg et al [65] noted that, since $\lambda_\alpha \gg \lambda_{sf}$ the above equation can be reduced to:

$$t_{(U/Xe)} = \frac{1}{\lambda_\alpha} \ln\left[\frac{{}^{A}Xe_{sf}\lambda_\alpha}{{}^{238}U^{A}Y_{sf}\lambda_{sf}} + 1\right].$$

Determining the relevant ages necessitates knowledge of the product of $\lambda_{sf}{}^{iA}Y_{sf}$, but values published for $\lambda_{sf}{}^{136}Y_{sf}$ scatter between 7.4×10^{-18}/a and 5.4×10^{-18}/a with most of the published λ_{sf}-values clustered around 6 and 9.10^{-17}/a. The yield of the main ^{238}U spontaneous fission isotope ^{136}Xe is roughly 6%. Because the rate of production ratio $^{136}Xe_{sf}/^{206}Pb_{rad}$ is of the order of 4.10^{-8}, the U/Xe method was applied initially to uranium-rich minerals such as pitchblende, but later uranium-poorer accessory minerals such as monazites and zircons have been investigated as well. Eikenberg et al [65] mentioned that pitchblendes are liable to be affected by geological events causing alteration or dissolution and subsequent re-distribution of uranium and its daughters so that it is the case that the reported U/Xe ages of pitchblendes are frequently lower than their formation ages. Earlier, this disparity was ascribed to gas losses by diffusion from which it could be inferred that pitchblende is unsuited for dating by the U/Xe approach. Later work using the U/Xe, U/Kr and U/Pb systems together with electron microprobe analysis demonstrated that the fission gases in pitchblendes could well have survived even greenschist facies metamorphism so that studying them would aid in the interpretation of diacordant U/Pb isotope ages. Obviously if geologically undisturbed pitchblendes gave concordant U/Pb ages and underwent no losses of fission gases, the U/Xe and U/Kr ages should both be identical and agree with the U/Pb ages if appropriate values for λ_{sf}, ${}^{i}Y_{sf}$ and $(^{136}Xe/^{86}Kr)_{sf}$ are employed. Where gas losses did occur, however, krypton seems always to be lost preferentially with respect to xenon and both fissiogenic xenon and Pb losses ran almost parallel. Discordant fission gas ages, that is to say $^{136}Xe_{sf}/^{86}Kr_{sf} \geq \pm6.1\pm0.1$, clearly indicate perturbation of the U/Pb system. Also, extensive fractionation between Xe and Kr in pitchblendes has been observed. Eikenberg et al [65] attempted to deduce a value for $\lambda_{sf}{}^{136}Y_{sf}$ as well as the isotopic composition of spontaneous fission Xe and krypton together with the spontaneous fission $^{136}Xe/^{86}Kr$ ratio. They analyzed two types of pitchblende, coarse-grained and finely disseminated, applying U/Pb analysis, noble gas analysis, electron microprobe and atomic absorption analysis, obtaining important data. Some samples gave discordant U/Pb, but concordant U/Xe and U/Kr, ages coinciding with lower U/Pb discordia intercepts and U/Pb microprobe ages from single grains. They contained pitchblende as fine-grained, ore disseminations probably representing recrystallized minerals. In the course of dissolution and precipitation of U, fission gases were released quantitatively from the system which produced a resetting of the U-Xe-Kr clock. Parts of radiogenic Pb still occurred in minerals adjacent to pitchblende.

In the samples of Eikenberg et al [65], Xe and Kr constituted mixtures from 4 sources, namely (1) the spontaneous fission of ^{238}U, (2) the slow neutron-induced fission of ^{235}U, (3) the fast neutron-induced fission of ^{238}U and (4) atmospheric gases. Atmospheric Xe and Kr impurities were removed by the assumption that ^{130}Xe and ^{82}Kr are wholly atmospheric. This was justified on the basis that these isotopes are shielded by the stable isobars ^{130}Te and ^{82}Se, respectively, also because the direct fission yields of both are below 0.01%. And as the measured $^{130}Xe/^{136}Xe$ ratio was usually less than 10^{-2} and in most cases below 10^{-3}, probably very little contamination with atmospheric Xe takes place. However, contamination of samples with atmospheric Kr was regarded as graver than Xe since the atmosphere contains approximately an order of magnitude more Kr than Xe. In addition, the fission yields of ^{84}Kr and ^{83}Kr are *ca* 40 and 150 times lower than those of ^{136}Xe. Luckily, most samples were only very slightly contaminated with atmospheric Kr as demonstrated by their low $^{82}Kr/^{86}Kr$ ratios.

To use the U/Xe/Kr dating method, the product $\lambda_{sf}{}^{i}Y_{sf}$ must be known. Additionally, so should the concentrations of spontaneous fission Xe and Kr, the relative Xe and Kr spontaneous fission yields and the $(^{136}Xe/^{86}Kr)_{sf}$ ratio. Any contribution from ^{238}U which underwent fast neutron-induced fission can be neglected. Eikenberg et al [65] commenced their iteration with the following values; for ${}^{136}Y$ from the slow neutron-induced fission of ^{235}U 6.39% and for ${}^{136}Y_{sf}$ 6.3%, both taken from earlier researchers. Other germane values were adopted from them as well. From isotope pairs 136–131, 134–131 and 132–131 for which the differences between induced and spontaneous composition are large, a mean value for a factor R was calculated for each sample, R being the ratio of induced to spontaneous fission events. Then $U/^{i}Xe$ and $U/^{i}Kr$ ages for each sample were calculated. While the $U/^{i}Xe$ ages were only slightly different, there were significant

differences between the U/^{136}Xe and U/^{86}Kr ages ef geologically unaffected pitchblendes, a matter regarded as unsurprising by Eikenberg et al [65] on the grounds that varying compositions of fission Kr from $^{238}U_{sf}$ have been reported. Keeping $^{136}Y_{sf}$ fixed, they changed the $^{i,j}Y_{sf}$ yields of the deviational U/^{i}Xe and U/^{i}Kr systems to obtain agreement between all ages ($^{i,j}Y_{sf}$ being the mass yields of the isotopes i and j from ^{238}U spontaneous and ^{235}U slow neutron fission, respectively). The new yields were inserted into suitable equations so as to calculate a new set of ages, a procedure iterated until all ages agreed satisfactorily within analytical error. Most samples gave $(^{136}Xe/^{86}Kr)_{sf}$ values around 6.1. And back-up data showed that they were not geologically disturbed. However, some samples had undergone Xe, Kr and Pb losses up to 50% – but they were still suitable to determine the relative $^{i}Xe_{sf}$ and $^{i}Kr_{sf}$ isotopic ratios. This is because minute losses of noble gases have an undetectable effect on the isotopic composition of Xe and Kr. As regards such geologically undisturbed samples, the product $\lambda_{sf}{}^{136}Y_{sf}$ was obtained and required that the minerals analyzed remained closed both to U and the fission gases. Only samples with concordant U/Pb ages and the recrystallized pitchblendes (U/Pb discordant, but U/Xe/Kr concordant) were examined, the latter having formation ages determinable from the intercept of the U/Pb discordia with the concordia and also from U/Pb microprobe analysis. All values of $\lambda_{sf}{}^{136}Y_{sf}$ were around $5.7 \cdot 10^{-18}$/a and agreed within error. No fractionation between the heavier xenon and the lighter krypton was observed from which it was concluded that the selected minerals retained their fission Xe quantitatively. Comparing the value for $\lambda_{sf}{}^{136}Y_{sf}$ obtained with values given using other techniques such as radiochemical isotope counting and fission track methods gave interesting results. For λ_{sf}, there are two widely used values, one derived from direct fission counting which is $8.5 \cdot 10^{-17}$/a and a second based on fission track results which is $6.4 \cdot 10^{-17}$/a. Refining the value was achieved by fitting spontaneous fission mass yield data from various sources and this produced $(8.6 \pm 0.2) \cdot 10^{-17}$/a. This last was published by von Gunten [66]. Considering his figure and fission yields given by Kuroda et al [67], a value for $\lambda_{sf}{}^{136}Y_{sf}$ of $5.4 \cdot 10^{-18}$/a can be obtained and this compares well with the Eikenberg et al [65] value of $(5.7 \pm 0.4) \cdot 10^{-18}$/a, and these researchers noted that using a lower value of $\lambda_{sf} = 6.4 \cdot 10^{-17}$/a would require $^{136}Y_{sf} = 9\%$ to accord with their result. They added that such a large ^{238}U fission yield at mass 136 is impossible because it would entail a total mass yield beyond 100% taking the relative yields from Kuroda et al [67] or von Gunten [66]. They concluded that their work and earlier studies on uranium-bearing minerals demonstrated that the high value of $8.6 \cdot 10^{-17}$/a for λ_{sf} is correct, but a discrepancy of ~20% remains between the $\lambda_{sf}{}^{'}Y_{sf}$ values found from U minerals e.g. pitchblende or uraninite on the one hand and uranium-bearing accessory minerals such as zircon or monazite on the other. Taking the most commonly utilized value of 6.3% for $^{136}Y_{sf}$ and the high value of $7.4 \cdot 10^{-18}$/a for $\lambda_{sf}{}^{136}Y_{sf}$, a value of $11.7 \cdot 10^{-17}$/a would result for λ_{sf} which is significantly greater than either the fission decay constants proposed by von Gunten [66] or Fleischer and Price [68]. Such a result would not accord with almost all values for λ_{sf} obtained from various methods.

Eikenberg et al [65] investigated the isotopic composition of spontaneous fission Xe and Kr, noting that their isotopic abundances of ^{238}U-derived Xe_{sf} were close to previously published values with a small depletion of the lighter fission Xe isotopes relative to $^{136}Xe_{sf}$. They noted that Shukolyukov [69] measured Xe in samarskite and recorded a fissiogenic Xe and Kr composition close to theirs, adding that this mineral has high REE concentrations and apparently the high neutron absorption cross-sections of several REE isotopes favour the mineral in studying the spontaneous fission Xe and Kr isotope spectrum.

Leaving aside the samarskite case, the isotope ratios for spontaneous fission Kr presented disagree with values reported earlier. However, all data defined a linear array extrapolating through a calculated spontaneous fission point as well as a ^{235}U slow neutron-induced fission point given by Crough [70]. Eikenberg et al [65] took this as indicative that, like Xe, fission Kr in their samples comprises two components, i.e. spontaneous fission of ^{238}U and slow neutron-induced fission of ^{235}U. Results showed strong support for the validity of the isotopic composition of fissiogenic Kr from $^{238}U_{sf}$.

Regarding the ^{138}Xe/^{86}Kr spontaneous fission ratio, these researchers noted that nine undisturbed samples having minor contribution of induced fission krypton ($R \leq 0.05$) gave $(^{136}Xe/^{86}Kr)_{sf}$ ratios which ranged from 5.9 to 6.3 with a mean value of 6.1 ± 0.1. This agreed well with a zircon-derived value of 6.0 ± 0.4 given by Hebeda et al [71]. Some samples lost fissiogenic daughter products which caused fractionation between Xe and Kr, thus raising $(^{136}Xe/^{86}Kr)_{sf}$ ratios. The U/Pb concordant uraninite B–1 gave a surprisingly high $(^{136}Xe/^{86}Kr)_{sf}$ ratio of 6.5. As

this particular sample was much the oldest uranium-rich sample at *ca* 1.5 Ga, probably the long self-irradiation gave rise to lattice deformations resulting in a small Kr loss of 6%. Eikenberg et al. [65] suggested that uranium-bearing minerals with $(^{136}Xe/^{86}Kr)_{sf}$ 6.1±0.1 show concordant U/Xe and U/Kr ages.

8.21.1. Fissiogenic rare cases in the atmosphere

Eikenberg et al. [65] estimated a maximum contribution of ^{136}Xe from ^{238}U spontaneous fission of 1.6% to the total inventory of to the total inventory of ^{136}Xe in the atmosphere which agees with estimates given by Pepin and Phinney [72] and Bernatowicz and Podosek [73]. The source for ^{129}Xe is not yet established, but excess of it has been recorded in terrestrial gases and minerals, for instance by Staudacher and Allègre [74]. Such excesses may be due to the production of now extinct ^{129}I ($T_{1/2}$ = 16 Ma) during nucleosynthesis or perhaps arose from a non-primordial origin. However, Eikenberg et al. [75] ruled out significant contribution of ^{129}Xe from $^{238}U_{sf}$ to the Earth's atmosphere on the basis of their $^{129}Xe/^{136}Xe$ spontaneous fission ratio of ≤ 0.001.

8.22. REFERENCES

1. C. M. Merrihue, G. Turner, J. Geophys. Res., 71, 2852 (1966)
2. G. Turner, in Meteorite Research ed. P. M. Millman, Reidel Publishing Co., Dordrecht, 407 (1969)
3. G. B. Dalrymple, US Geol. Surv. Bull., 1890, 89 (1989)
4. M. J. Kunk, L. W. Snee, B. M. French, S. S. Harlan, J. J. McGee, Lunar and Planetary Sciences XXIV, Part 1 A–F, Lyndon B. Johnson Space Center, Houston, 835 (1993)
5. J. D. Blum, C. Pege Chamberlain, M. P. Hingston, C. Koeberl, L. E. Marin, B. C. Schuraytz, V. L. Sharpton, Nature, 364, 325 (1993)
5. T. Lee, T.-L. Ku, H.-L. Lu, J.-C. Chen, First detection of fallout Cs-135 and potential applications of $^{137}Cs/^{135}Cs$ ratios. Geochim. Cosmochim. Acta, 57, 3493–3497 (1993)
6. D. Lal, B. L. K. Somanyajulu, Tectonophysics, 105, 383 (1984)
7. D. K. Pal, C. Tuniz, R. K. Moniot, T. H. Kruse, G. F. Herzog, Science, 218, 787 (1982)
8. D. Lal, S. Peters, in Handbuch der Physik ed. K. Sitte, Springer-Verlag, Berlin, 351 (1967)
9. H. W. Bentley, F. M. Phillips, S. N. Davis, in Handbook of Environmental Geochemistry, Vol. 2, The Terrestrial Environment ed. P. Fritz, J.-C. Fontes, Elsevier, Amsterdam, 427 (1986)
10. D. Elmore, L. E. Tubbs, D. Newman, X. Z. Ma, R. Finkel, K. Nishiisumi, J. Beer, H. Oeschger, M. Andree, Nature, 300, 735 (1982)
11. L. Carlsson, T. Olsson, J. N. Andrews, J.-G. Fontes, J. L. Michelot, K. Nordstrom, SKBF/KBS Prog. Rept 83–01, Stockholm (1983)
12. M. W. Kuhn, S. N. Davis, H. W. Bentley, R. Zito, Geophys. Res. Letts, 11, 607 (1984)
13. V. V. Kuzimov, A. A. Pomansky, Radiocarbon, 22, 311 (1980)
14. D. E. Alburger, G. Harbottle, E. F. Norton, Earth Planet. Sci. Lett., 78, 168 (1986)
15. A. L. Odom, W. J. Rink, Geology, 17, 55 (1988)
16. A. J. Hurford, P. F. Green, Earth Planet. Sci., Lett., 59, 343 (1983)
17. P. F. Green, Isotope Geoscience, 58, 1 (1985)
18. P. K. Zeitler, N. M. Johnson, G. W. Maeser, R. A. K. Tahirkeli, Nature, 298, 255 (1982)
19. A. J. W. Gleadow, I. R. Duddy, P. L. Green, K. A. Hegarty, Earth Sci. Planet. Lett., 78, 245 (1986)
20. P. J. Patchett, M. Tatsumoto, Cont. Min. Pet., 78, 279 (1981)
21. H. S. Pettingell, P. J. Patchett, M. Tatsumoto, S. Moorbath, Earth Planet. Sci. Lett., 55, 150 (1981)
22. P. J. Patchett, M. Tatsumoto, Geophys. Res. Letts, 7, 1077 (1980)
23. Q. Z. Yin, E. Jagoutz, A. B. Yerkhovskiy, H. Wänke, Geochim. Cosmochim. Acta, 57, 4119 (1993)
23. K. H. Rubin, J. D. Macdougall, M. R. Perfit, ^{210}Po–^{210}Pb dating of recent volcanic eruptions on the sea floor. Nature, 368, 841–844 (1994)
24. J. C. Roddick, Earth Planet, Sci. Lett., 12, 300 (1983)
25. T. J. Dempster, Earth Planet. Sci. Lett., 78, 355 (1986)
26. C. Chopin, H. Maluski, Cont. Min. Pet., 74, 109 (1980)
27. R. H. Verschure, P. A. M. Andriessen, N. A. I. M. Boelrijk, E. H. Hebeda, C. Maijer, H. N. A. Priem, E. A. Th. Verdurmen, Cont. Min. Pet., 74, 245 (1980)
28. A. L. Armstrong, in Potassium-Argon Dating ed. D. A. Schaeffer, J. Zahringer, Springer-Verlag, New York, 117 (1966)
29. C. H. Stockwell, Geol. Surv. Canada, Paper 80–19, Part 1, 135 pp (1982)
30. B. D. Marshall, D. J. DePaolo, Geochim. Cosmochim. Acta, 46, 2537 (1982)
31. P. H. Fowler, A. R. Lang, Nature, 270, 163 (1977)
32. S. R. Hashemi-Nezhad, J. H. Fremlin, S. A. Durrant, Nature, 278, 333 (1979)
33. J. R. Arnold, W. F. Libby, Science, 110, 678 (1949)
34. I. Karlen, I. U. Olsson, P. Kalberg, S. Kilicci, Arkiv. Geofysik., 6, 465 (1966)

35. H. Godwin, Nature, 195, 984 (1962)
36. H. De Vries, proc. Koninkl. Ned. Akad. Wetenschap., B61, 94 (1958)
37. H. E. Suess, Science, 122, 415 (1955)
38. K. O. Münnich, Naturwiss., 44, 32 (1957)
39. C. R. Gleidmþin, G. A. Jones, J. Geophys. Res., 98, 14557 (1993)
40. E. R. M. Druffel, S. Griffin, J. Geophys. Res., 98, 20249 (1993)
41. J. M. Luck, L. Birck, C. J. Allègre, Nature, 283, 256 (1980)
42. K. Bell, J. L. Powell, J. Petrol., 10, 536 (1969)
43. D. A. Papanastassiou, G. J. Wasserburg, Eartl Planet. Sci. Lett., 5, 361 (1969)
44. L. E. Nyquist, Phys. and Chem. of the Earth, 10, 103 (1977)
45. P. J. Hamilton, N. M. Evensen, R. K. O'Nions, H. S. Smith, A. J. Erlank, Nature, 277, 325 (1979)
46. A. G. Wintle, J. A. Westgate, Geology, 14, 594 (1986)
47. J. A. Strain, P. D. Townsend, B. Jassemnjad, S. W. S. McKeever, Earth Planet. Sci. Lett., 77, 14 (1986)
48. D. Lal, H. E. Suess, Ann. Rev. Nucl. Sci., 18, 407 (1968)
49. L. L. Thatcher, B. R. Payne, Proc. 6th Internat'l Conf. Radiocarbon and Tritium Dating, Pullman, Washington, 604 (1965)
50. T. Dinçer, G. H. Davis, Proc. 8th Cong. Internat'l Assoc. Hydrogeol., Istanbul, Turkey, 276 (1967)
51. G. B. Allison, M. W. Hughes, Proc. Interpretation of Environmental Isotopes and Hydrochemical Data, Vienna, Austria, IAEA, SM/182/4, ,57 (1976)
52. M. Bernat, C. J. Allegre, Earth Planet. Sci. Lett., 21, 310 (1974)
53. M. S. Baxter, R. W. Crawford, D. S, Swan, J. G. Farmer, Earth Planet. Sci. Lett., 53, 434 (1981)
54. W. S. Broecker, J. Geophys. Res., 68, 2817 (1963)
55. M. Milankovitch, Theorie Mathematique des Phenomenes Thermiques produits par la radiation solaire. Gauthier-Villaris, Paris (1920)
56. D. L. Thurber, J. Geophys. Res., 67, 4318 (1962)
57. J. Kronfeld, E. Rosenthal, J. Hydrol., 50, 179 (1981)
58. S. S. Goldich, M. G. Mudrey Jnr, in Cont. to recent geochemistry and analytical chemistry, A. P. Vinogradov Volume.ed. A. I. Tugarinov, Nauka Publ. Office, Moscow, 415 (1972)
59. A. Holmes, Nature, 157, 680 (1946)
60. F. G. Houtermans, Naturwiss., 33, 185 (1946)
61. R. D. Russell, R. M. Farquhar, Lead isotopes in Geology, Interscience Publishers, New York (1960)
62. R. A. Alpher, R. C. Herman, Phys. Rev., 84, 1111 (1951)
63. V. G. Khlopin, E. K. Gerling, N. V. Baruiovaknya, (1947). The presence of certain stable products of the spontaneous disintegration of uranium in nature. Bull. Acad. Sci. Chim., 599–604 (in Russian).
64. J. MacNamara, H. G. Thode, (1950). The isotopes of xenon and krypton in pitchblende and the spontaneous fission of uranium. Phys. Rev., 80, 471–472.
65. J. Eikenberg, P. Signer, R. Wieler, (1993). U–Xe, U–Kr and U–Pb systematics for dating uranium minerals and investigations of the production of nucleogenic neon and argon. Geochimica et Cosmochimica Acta, 57, 1053–1069.
66. von Gunten, H. R. (1969). Distribution of mass in spontaneous and neutron-induced fission. Actinide Rev., 1, 275–298.
67. P. K. Kuroda, R. R. Edwards, F. T. Ashizawa, (1956). Radiochemical measurements of the natural fission rate of uranium and the natural occurrence of short-lived iodine isotopes. J. Chem. Phys., 25, 603–609.
68. R. L. Fleischer, B. P. Price, (1964). Decay constant for spontaneous fission Phys. Rev., 133, B63–B64.
69. Shukolyukov, Yu. A. (1970). The decay of uranium nuclei in nature. Atomizdat Publisky, Moskva (in Russian).
70. E. A. C. Crough, (1977). Fisson Product Yields from Neutron-Induced Fission. Atomic Data and Nuclear Data Tables. Harwell Acad. Press.
71. E. H. Hebeda, M. Freudel, L. Schultz (1987). Radiogenic, fissiogenic and nucleogenic noble gases in zircons. Earth Planet. Sci. Lett., 85, 79–90.
72. Pepin, R. O., Phinney, D. (1976). The formation interval of the earth. Lunar Sci., VII, 682–684.
73. T. J. Bernatowicz, F. A. Podosek, (1978). Nuclear components in the atmosphere. In Terrestrial Rare Gases, ed. E. C. Alexander, M. Ozima, Scientific Society Press, Japan, 99–135.
74. Staudacher, T., Allegre, C. J. (1982). Terrestrial xenology. Earth Planet. Sci. Lett., 60, 389–406.
75. W. H. Fleming, H. G. Thode, (1953). Neutron and spontaneous fission in uranium ores. Phys. Rev., 90, 378–382.